

Article

An Efficient Electric Charged Particles Optimization Algorithm for Numerical Optimization and Optimal Estimation of Photovoltaic Models

Salah Kamel ¹, Essam H. Houssein ², Mohamed H. Hassan ¹, Mokhtar Shouran ^{3,*} and Fatma A. Hashim ⁴

¹ Department of Electrical Engineering, Faculty of Engineering, Aswan University, Aswan 81542, Egypt; skamel@aswu.edu.eg (S.K.); mohamed.hosny@moere.gov.eg (M.H.H.)

² Faculty of Computers and Information, Minia University, Minia 61519, Egypt; essam.halim@mu.edu.eg

³ Wolfson Centre for Magnetics, School of Engineering, Cardiff University, Cardiff CF24 3AA, UK

⁴ Faculty of Engineering, Helwan University, Cairo 11795, Egypt; fatma_hashim@h-eng.helwan.edu.eg

* Correspondence: shouranma@cardiff.ac.uk

Abstract: The electric charged particles optimization (ECPO) technique is inspired by the interaction (exerted forces) between electrically charged particles. A developed version of ECPO called MECPO is suggested in this article to enhance the capability of searching and balancing the exploitation and exploration phases of the conventional ECPO. To let the search agent jumps out from the local optimum and avoid stagnation in the local optimum in the proposed MECPO, three different strategies in the interaction between ECPs are modified in conjunction with the conventional ECPO. Therefore, the convergence rate is enhanced and reaches rapidly to the optimal solution. To evaluate the effectiveness of the MECPO, it is executed on the test functions of the CEC'17. Furthermore, the MECPO technique is suggested to estimate the parameters of different photovoltaic models, such as the single-diode model (SDM), the double-diode model (DDM), and the triple-diode model (TDM). The simulation results illustrate the validation and effectiveness of MECPO in extracting parameters from photovoltaic models.

Keywords: electric charged particles optimization (ECPO); CEC 2017 test suite; PV parameter estimation; single-diode model; double-diode model; triple-diode model; solar energy

MSC: 65K10-91B74-00A69



Citation: Kamel, S.; Houssein, E.H.; Hassan, M.H.; Shouran, M.; Hashim, F.A. An Efficient Electric Charged Particles Optimization Algorithm for Numerical Optimization and Optimal Estimation of Photovoltaic Models. *Mathematics* **2022**, *10*, 913. <https://doi.org/10.3390/math10060913>

Academic Editor: Armin Fügenschuh

Received: 10 February 2022

Accepted: 9 March 2022

Published: 13 March 2022

Publisher's Note: MDPI stays neutral with regard to jurisdictional claims in published maps and institutional affiliations.



Copyright: © 2022 by the authors. Licensee MDPI, Basel, Switzerland. This article is an open access article distributed under the terms and conditions of the Creative Commons Attribution (CC BY) license (<https://creativecommons.org/licenses/by/4.0/>).

1. Introduction

To deal with the increase in energy shortage as well as the several disadvantages of fossil fuels, increased research studies on renewable energy sources (RES) are urgently required [1,2]. Solar energy is one of the most important RES that researchers focus on due to its many advantages such as cleanliness, safeness, and abundance [3]. The principal kind of solar energy is photovoltaic power generation [4]. PV solar installations around the world increased from about 217 GW in 2015 to just over 707 GW in 2020 [5]. However, using photovoltaic systems to produce electric energy is a big challenge because of their reliance on the climate and other factors [1]. Consequently, a precise model that almost represents the non-linear current–voltage (I–V) and the power–voltage (P–V) output characteristics of the PV model under normal operation is required for simulation and evaluation of photovoltaic systems [6]. These non-linearity challenges are difficult for any possibility and approximation to boost efficiency [7].

A solar PV cell is the main unit of the photovoltaic system. Therefore, it is important to estimate its unknown parameters to acquire a relative analysis of the PV panel performance. The equivalent circuits for the single-, double- and triple-diode model for parameter identification are well-known and most extensively used ways [8,9]. There are five parameters required in the single-diode model (SDM), while there are seven unknown parameters in

the double-diode model (DDM) and nine unknown parameters in the triple-diode model (TDM). In many works of literature, the SDM and DDM are generally employed, in which the researchers have used several techniques to estimate the parameters of the PV model based on analytical and numerical methods and optimization techniques [10,11]. Despite the analytical approaches are the simplest and they reach the result rapidly, they do not have the precision under normal conditions [7].

Several metaheuristic techniques have been improved and employed to reach the optimum solution for the PV parameters extraction problem. An artificial electric field algorithm (AEFA) was proposed to extract nine parameters of the triple-diode photovoltaic model [12]. Meiyang Ye employed the particle swarm algorithm (PSO) to solve the solar cell parameters [13]. In [14], the direction of movement (DM) in the gradient-based optimizer (GBO) algorithm is used to converge around the area of the solution, and it was suggested to change the DM value gradually in the modified gradient-based optimizer (MGBO) to improve the balancing between exploration and exploitation phases in the search process. The flower pollination algorithms (FPA) were used to extract the global parameters of both the single-diode and the double-diode models based on the experimental data [15]. Additionally, other recent optimization algorithms were used to find the best values of PV parameters, including transient search optimization (TSO) [16], cuckoo search (CS) [17], whale optimization algorithm (WOA) [18], supply demand-based optimization (SDO) [19], salp swarm algorithm (SSA) [20], improved bonobo optimizer (IBO) [21], multiverse optimizer (MVO) [22], tree growth algorithm (TGA) [23], grey wolf optimization (GWO) [24], triple-phase teaching-learning-based optimization (TPTLBO) [25], ant lion optimization (ALO) [26], chaos game optimization (CGO) [27], Harris hawk optimization (HHO) [28], Rao algorithm [29], slime mould algorithm (SMA) [30], and hybrid techniques, such as hybrid adaptive TLBO with DE algorithm (ATLDE) [31], GWOCS [1], PSOGWO [32], Marine predator algorithm (MPA) [33], Coyote optimization [34], and Jaya algorithm and its variants [35]. Each technique has various strategies to achieve a certain objective, and the power of each technique depends on the precision of the estimated parameters, computation time, and computational complexity.

In this article, a development version of ECPO called MECPO is suggested to enhance the search capability of searching and to increase the balance between the exploitation and exploration for the conventional ECPO. In addition, this new algorithm is utilized for extracting the PV module parameters. The performance of the MECPO technique is compared with the recent techniques, such as COOT [36], equilibrium optimizer (EO) [37], Giza pyramids construction (GPC) [38], and MPA [39] algorithms, as well as the original ECPO algorithm [40]. However, the major contributions of this paper are summarized as follows:

- Proposing an effective optimizer called MECPO with the aim of improving the performance of the original algorithm.
- The CEC'17 test suite is used to assess the MECPO efficiency.
- The proposed MECPO algorithm is employed for the PV models: SDM, DDM, and TDM of PV modules.
- The obtained statistical results using the proposed algorithm are compared with state-of-the-art techniques.
- The superiority and reliability of the MECPO-based methodology in solving the parameter estimating for the PV model's problem are verified.

The rest of the article is organized as follows: Section 2 of the paper analyzes the problem formulation, including SDM, DDM, and TDM, and presents the objective function for identifying the parameters of the solar PV module. Section 3 presents an overview of the ECPO technique and the proposed MECPO technique. Section 4 describes the results, discussions, and comparisons. Section 5 gives the conclusion of this article with the final remarks.

2. PV Models

In this section, the PV models are presented. The PV models include the single-diode model (SDM), the double-diode model (DDM), and the triple-diode model (TDM).

2.1. Single-Diode Model (SDM)

SDM is simple, and Figure 1 illustrates its equivalent circuit diagram. In this figure, there are many significant parameters such as photocurrent I_{Ph} , the current of diode I_{D1} , shunt resistance R_{sh} , series resistance R_s , and output current I . It is observed from Figure 1 that it is easy to compute the output current for this model as follows:

$$I = I_{Ph} - I_{D1} - I_{sh} \quad (1)$$

where I_{sh} is the shunt resistor current.

The modeling of SDM is represented in the following equation:

$$I = I_{Ph} - I_{sd} \left[\exp \left(\frac{q(V + IR_s)}{NKT} \right) - 1 \right] - \frac{V + IR_s}{R_{sh}} \quad (2)$$

where

- I_{sd} is the reverse saturation current of D_1 .
- The variable $q = 1.60217646 \times 10^{-19}$ C is the charge of the electron.
- V is the total voltage.
- $K = 1.3806503 \times 10^{-23}$ (J/k) is the Boltzmann's constant.
- T is the temperature in Kelvin.
- N is the ideality factor of D_1 .

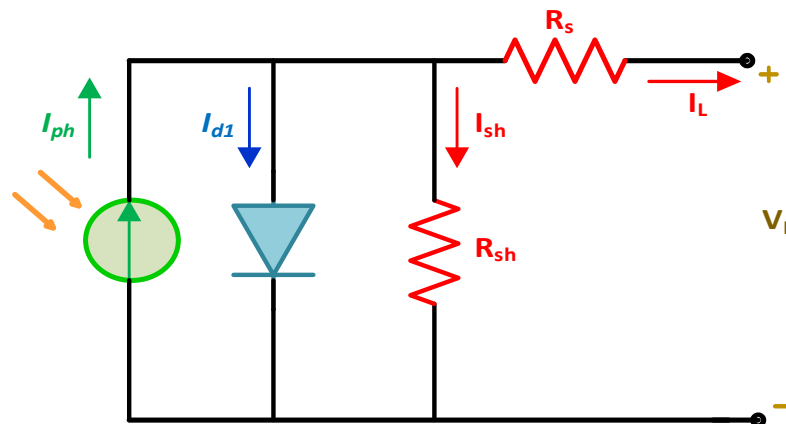


Figure 1. SDM mathematical model.

2.2. The Double-Diode Model (DDM)

Compared to the first case (SDM), the impact of compound current loss is taken into consideration in the DDM. Figure 2 displays the structure of DDM. It can be seen from this figure that there are two diodes, in this case, in parallel with the source of current. The output current of the DDM is calculated from the following equation:

$$I = I_{Ph} - I_{D1} - I_{D2} - I_{sh} \quad (3)$$

$$I = I_{Ph} - I_{sd1} \left[\exp \left(\frac{q(V + IR_s)}{N_1 KT} \right) - 1 \right] - I_{sd2} \left[\exp \left(\frac{q(V + IR_s)}{N_2 KT} \right) - 1 \right] - \frac{V + IR_s}{R_{sh}} \quad (4)$$

where

- I_{sd1} and I_{sd2} are the reverse saturation current of D_1 and D_2 , respectively.
- N_1 and N_2 are the ideality factor of D_1 and D_2 , respectively.

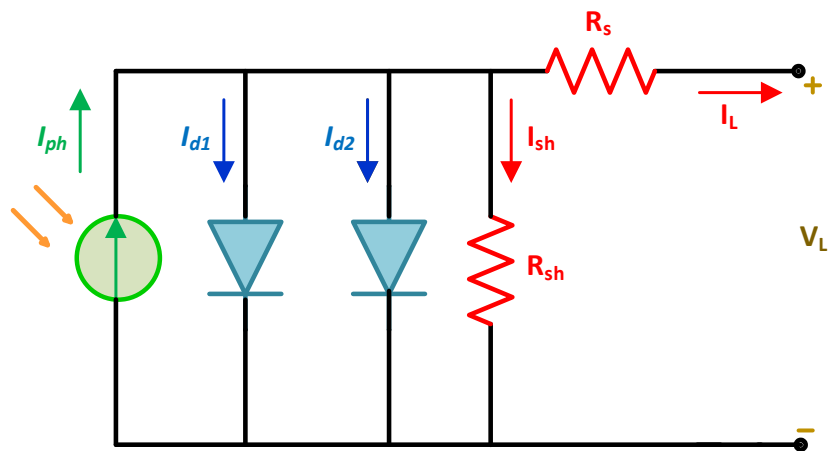


Figure 2. DDM mathematical model.

2.3. The Triple-Diode Model (TDM)

TDM has three diodes in parallel with the current source, as shown in Figure 3. Therefore, the output current can be given by the following equations:

$$I = I_{Ph} - I_{sd1} - I_{sd2} - I_{sd3} - I_{sh} \quad (5)$$

$$I = I_{Ph} - I_{sd1} \left[\exp\left(\frac{q(V + IR_S)}{N_1 KT}\right) - 1 \right] - I_{sd2} \left[\exp\left(\frac{q(V + IR_S)}{N_2 KT}\right) - 1 \right] - I_{sd3} \left[\exp\left(\frac{q(V + IR_S)}{N_3 KT}\right) - 1 \right] - \frac{V + IR_S}{R_{sh}} \quad (6)$$

where

- I_{sd1} , I_{sd2} , and I_{sd3} are the reverse saturation current of D_1 , D_2 , and D_3 , respectively.
- N_1 , N_2 , and N_3 are the ideality factor of D_1 , D_2 , and D_3 , respectively.

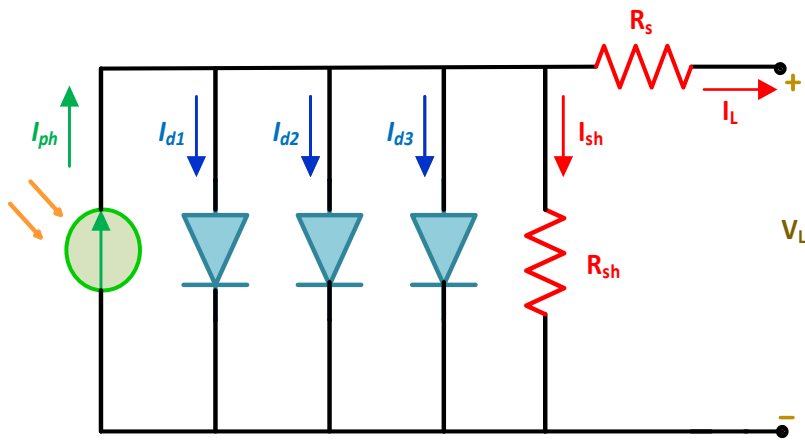


Figure 3. TDM mathematical model.

2.4. The Objective Function

The objective function is to extract the best parameter values of the PV models by reducing the variance between the estimated data and the measured data. The objective function of SDM, DDM, and TDM is given as follows [33]:

1. The objective function of SDM is given as:

$$f_{SD}(V, I, x) = I - x_3 + x_4 \left[\exp\left(\frac{q(V + Ix_1)}{x_5 KT}\right) - 1 \right] - \frac{V + Ix_1}{x_2} \quad (7)$$

2. The objective function of DDM is given as:

$$f_{DD}(V, I, x) = I - x_3 + x_4 \left[\exp \left(\frac{q(V + Ix_1)}{x_6 KT} \right) - 1 \right] + x_5 \left[\exp \left(\frac{q(V + Ix_1)}{x_7 KT} \right) - 1 \right] - \frac{V + Ix_1}{x_2} \quad (8)$$

3. The objective function of TDM is given as:

$$f_{TD}(V, I, x) = I - x_3 + x_4 \left[\exp \left(\frac{q(V + Ix_1)}{x_6 KT} \right) - 1 \right] + x_5 \left[\exp \left(\frac{q(V + Ix_1)}{x_7 KT} \right) - 1 \right] + x_8 \left[\exp \left(\frac{q(V + Ix_1)}{x_9 KT} \right) - 1 \right] - \frac{V + Ix_1}{x_2} \quad (9)$$

where

- V and I values can be given from a solar cell.
- $x = [x_1, x_2, \dots, x_n]$ is the estimating parameters vector for n-parameters for each solar cell model and can be defined as:
 - (1) $x = [R_s, R_{sh}, I_{ph}, I_{sd}, n]$ for SDM.
 - (2) $x = [R_s, R_{sh}, I_{ph}, I_{sd1}, I_{sd2}, n_1, n_2]$ for DDM.
 - (3) $x = [R_s, R_{sh}, I_{ph}, I_{sd1}, I_{sd2}, I_{sd3}, n_1, n_2, n_3]$ for TDM.

The lower and upper boundaries of the unknown parameters are presented in Table 1.

Table 1. The limits of extracted photovoltaic parameters.

Parameter	Lower Limit	Upper Limit
I_{ph} (A)	0	1
$I_{sd1}, I_{sd2}, I_{sd3}$ (μ A)	0	1
R_s (Ω)	0	0.5
R_{sh} (Ω)	0	100
n_1, n_2, n_3	1	2

In this paper, the root mean square error (RMSE) is the error between the estimated and the measured data of the diode model. Therefore, The RMSE can be calculated from the following equation [41]:

$$RMSE = \sqrt{\frac{1}{N} \sum_{i=1}^N (f_h(V, I, x))^2} \quad (10)$$

where

- h is the solar cell model to be used.
- N identifies a set of samples is employed to verify the best optimum.

3. The Proposed MECPO

In this section, an overview of the MECPO algorithm is presented in detail, which improves the original ECPO as (1) a new parameter called transfer factor (TF) is added to transfer from exploration to exploitation and vice versa; (2) the three different strategies in the interaction between ECPs are modified to avoid gradually move closer to better individuals who easily make the algorithm stagnation in local optimum and convergence prematurely, and (3) the diversification phase is modified to let the search agent jumps out from local optimum and avoid stagnation in local optimum efficiently.

3.1. Advanced Transfer Factor (TF)

The balance between the exploration and exploitation phases is regarded as the major process to the success of any optimization algorithm and is controlled by a specific parameter. The performance of ECPO is affected by the transferring parameter from exploration

to exploitation, which is missing. To resolve this issue, the non-linear parameter called transfer factor (TF) is injection into ECPO as follows:

$$TF = C_1 \times \cos\left(1 - \frac{t}{T}\right)^{C_2} \quad (11)$$

where C_1 and C_2 are constant 3 and 0.25, respectively.

This enhances the switching phase between exploration and exploitation in a proper manner and maintains the diversity of the solutions.

3.2. Modified Interaction Phase

In this subsection, some setting will be proposed to avoid gradually moving closer to better individuals, which easily make the algorithm stagnation in local optimum and convergence prematurely.

3.2.1. Strategy 1

In this strategy, two new ECPs are created, called ECP_{1new1} and ECP_{1new2} , while i denotes the index of the chosen ECP). This results from three interacting ECPs.

For ECP_1 , ECP_2 , and ECP_3 :

Where ECP_1 is the best agent, ECP_2 is the second-best agent, and ECP_3 is the third-best agent.

ECP_1 is affected by ECP_2 and ECP_{best} to move from ECP to ECP_{1new1} . The total force exerts on ECP_1 become:

$$F = F_{21} + D \times F_{best1} \quad (12)$$

$D = \pm 1$ —this parameter is proposed to give high opportunities with different values on resulting F to give high opportunities to change the direction of agents that results in a good scan of the given search space in all possible directions.

The total force that pushes ECP_1 to the move to ECP_{1new1} and it illustrates as below:

$$\begin{aligned} ECP_{1new1} &= ECP_1 + F \\ &= ECP_1 + F_{best1} + F_{21} \\ &= ECP_1 + D \times TF \times \beta \times (ECP_{best} - ECP_1) + \beta \times (ECP_1 - ECP_2) \end{aligned} \quad (13)$$

where β is a random number. F_{21} refers to the force on ECP_1 of ECP_2 and F_{best1} is the force on ECP_1 of ECP_{best} .

Then, ECP_1 is affected simultaneously by ECP_3 and ECP_{best} to move to ECP_{1new2} .

$$ECP_{1new2} = ECP_1 + D \times TF \times \beta \times (ECP_{best} - ECP_1) + \beta \times (ECP_1 - ECP_3) \quad (14)$$

3.2.2. Strategy 2

To resolve the issue of the lack of interaction between ECP_{best} and the rest of ECPs, in the proposed method of three interacting ECPs, each ECP creates one new ECP called ECP_{1new} .

$$\begin{aligned} ECP_{1new1} &= ECP_1 + F \\ &= ECP_1 + F_{21} + F_{31} \\ &= ECP_1 + D \times TF \times \beta \times (ECP_1 - ECP_2) + \beta \times (ECP_1 - ECP_3) \end{aligned} \quad (15)$$

For ECP_2 : The second particle ECP_2 is influenced at the same time by the first and third particles (i.e., ECP_1 and ECP_3), which moves to ECP_{2new} . The resulting force to move ECP_1 to ECP_{1new} can be defined as:

$$\begin{aligned} F &= F_{12} + F_{32} \\ ECP_{2new1} &= ECP_2 + F \\ &= ECP_2 + F_{12} + F_{32} \\ &= ECP_2 + D \times TF \times \beta \times (ECP_2 - ECP_1) + \beta \times (ECP_2 - ECP_3) \end{aligned} \quad (16)$$

where F_{12} is the force of ECP_1 on ECP_2 , and F_{32} is the force of ECP_3 on ECP_2 .

For ECP_3 :

The ECP_3 is affected by ECP_1 and ECP_2 at the same time with the force given by:

$$\begin{aligned} F &= F_{13} + F_{23} \\ ECP_{3\text{new1}} &= ECP_3 + F \\ &= ECP_3 + F_{13} + F_{23} \\ &= ECP_3 + D \times TF \times \beta \times (ECP_3 - ECP_1) + \beta \times (ECP_2 - ECP_3) \end{aligned} \quad (17)$$

where F_{13} is the force of ECP_1 on ECP_3 and F_{23} is the force of ECP_2 on ECP_3 .

3.2.3. Strategy 3

In the previous strategies, new ECPs are generated. Illustratively, the three interacting ECPs ($nECP = 3$) will generate nine new ECPs (six ECPs from strategy 1 and three from strategy 2). In strategy 3, the equations defined in the previous two strategies are used.

3.3. Modified Diversification

The diversification phase updates the portion of ECPs population based on a variable called probability of diversification ($Pd = 0.2$). The new ECPs update their positions by selecting a random archive pool previously created. In the proposed enhancement, the new ECPs update their positions with five cases, including selecting a random archive pool, the remaining proposed four cases are (1) new ECPs update their positions based on boundary constraints to create new ECPS in new regions that may be not visited before; (2) new ECPs update their position with the best ECP in the population; (3) new ECPs update based on information from the archive and random ECPs with controlling parameter a_j that initializes with a random value and decreases with problem size by multiplying it with another random number $[0, 1]$; (4) the new ECPS will equal the old ECPs (no change).

The proposed diversification phase jumps out from the local optimum and avoids stagnation in the local optimum.

For $i = 1$: newECP

$$a_j = rand \quad (18)$$

For $j = 1$: ProblemSize

$$\text{newEPC}_{i,j} = \begin{cases} \text{newEPC}_{i,j} = L_j + r_1 \times (U_j - L_j) & r_2 < 0.3 \\ \text{newEPC}_{i,j} = ECP_{best,j} & r_2 < 0.4 \\ (1 - a_j) \times \text{archiveECP}_{K,j} + a_j \times \text{randECP}_j & r_2 < 0.5 \text{ where } a_j = a_j * rand \\ \text{newEPC}_{i,j} = \text{archiveECP}_{K,j} & r_2 < 0.8 \\ \text{newEPC}_{i,j} = EPC_{i,j} & \text{otherwise} \end{cases} \quad (19)$$

End If;

End For;

Eventually, the pseudo-code of the MECPO method is reported in Algorithm 1, while Figure 4 illustrates the flowchart.

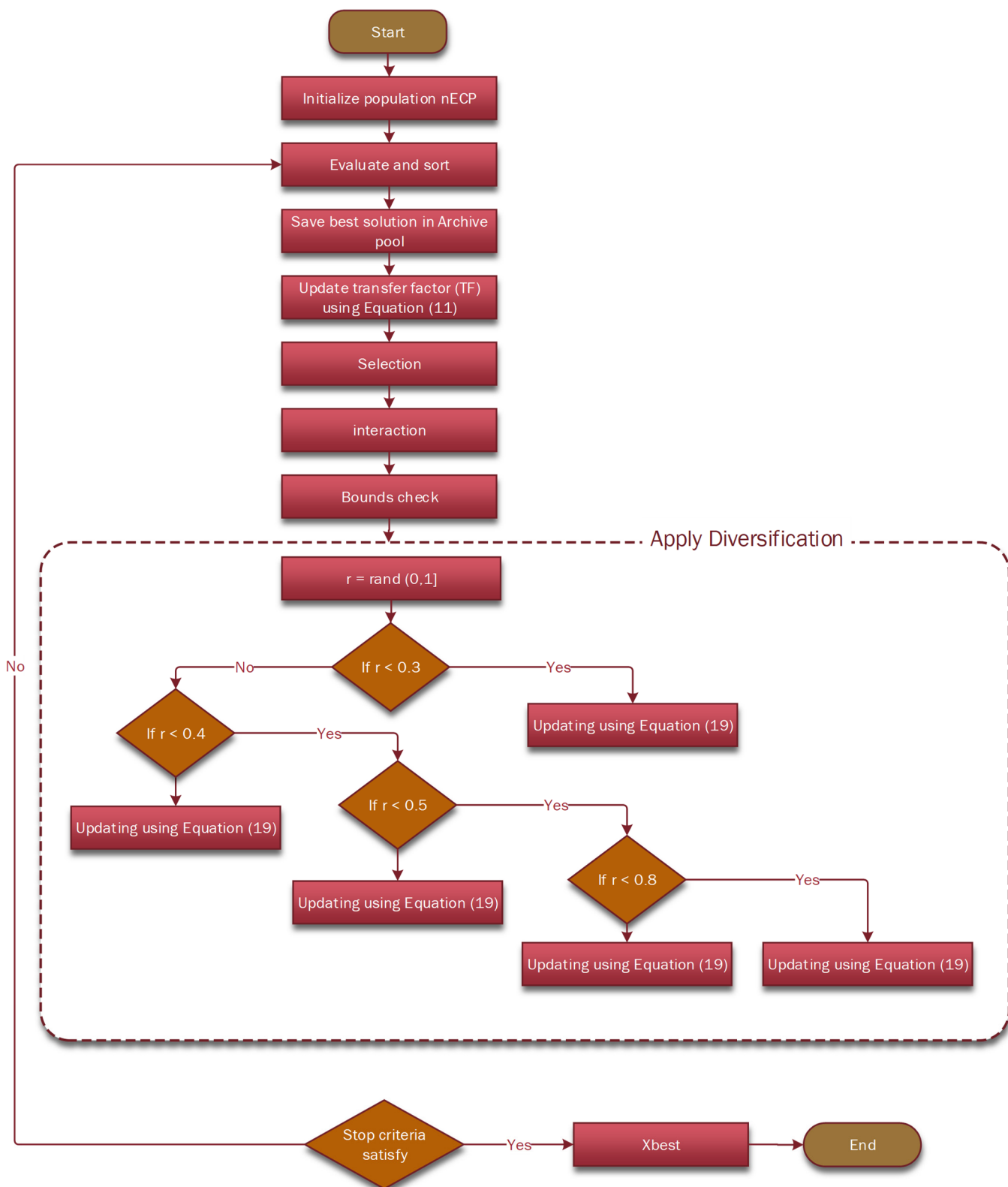


Figure 4. Flowchart of MECPO method.

Algorithm 1: Pseudo-code of the MECPO technique

```

1. Randomly initialize an nECP charged particles (solutions) using normal distribution
2. Calculate the fitness and sort them from the best to the worst
3. Create Archive pool with the best ECPs
4. Update transfer factor (TF) using Equation (11)
5. Selection: nECPI particles are randomly selected
6. Interaction: based on the specified strategy
   a. Strategy 1 using Equations (12)–(14)
   b. Strategy 2 using Equations (15)–(17)
   c. Strategy 3 using both of Strategy 1 and Strategy 2
7. For each individual  $X_i$ 
   if ( $X_i < X_{\min}$ )
       $X_i = X_{\min}$ 
   else if ( $X_{\max} < X_i$ )
       $X_i = X_{\max}$ 
   End If
   End For
8. Diversification
   a. For individual newECP (using Equation (19))
      ■ If  $r < 0.3$  then update its solution
      ■ Else If  $r < 0.4$  then update its solution
      ■ Else If  $r < 0.5$  then update its solution
      ■ Else If  $r < 0.8$  then update its solution
      ■ Else update its solution
   End If
End for
9. Termination criterion

```

4. Performance Evaluation of MECPO

To assess the performance of the MECPO technique, the 2017 IEEE Congress on Evolutionary Computation (CEC'17) test suite [42] is solved. In addition, several statistical metrics are extracted, including mean value and standard deviation (STD) for optimal values achieved. The achieved results are compared with seven recent metaheuristic techniques, for instance, gravitational search algorithm (GSA) [43], grey wolf optimizer (GWO) [44], WOA [45], sine cosine algorithm (SCA) [46], EO [37], HHO [47], and the original electric charged particles optimization (ECPO) [40].

4.1. Parameter Settings Values

Table 2 reports the parameters setting values; all the counterparts are evaluated on 30 independent runs and 1000 iterations (max_Itr) for every function for fair benchmarking comparison. We choose the default parameters values for the counterparts to decrease the risk of bias in the comparison, as illustrated in [48].

4.2. Definition of CEC'17 Benchmark Functions

CEC'17 test suite [42] including 29 functions is divided into three categories: (1) unimodal functions (F1–F3) has a single optimum solution and is used to evaluate the exploitation capability; (2) multimodal functions, which are from function F4 to function F10, have multiple local minima, and are employed to test the exploration capability; (3) hybrid functions from F11 to F20, and finally, the composition functions, which are from function F21 to function F30, have a huge number of local minima and are employed to evaluate the capability of the technique to avoid the local minima and try to maintain the stability between exploitation and exploration stages.

Table 2. The settings of the parameter for the MECPO technique and the counterparts.

Techniques		The Setting of Parameters
Public settings		Number of independent runs: 30 Maximum iterations: 1000 Population size: N = 30 Dim = 30,
GSA		$\alpha = 20$, $G_0 = 100$, $R_{norm} = 2$, $R_{power} = 1$
GWO		a linearly decrease from 2 to 0
WOA		α 2 linearly decreases from -1 to -2 α variable decreases linearly from 2 to 0
SCA		$A = 2$
EO		$a_1 = 2$, $a_2 = 1$, $GP = 0.5$
HHO		$E_0 \in [-1, 1]$, $\beta = 1.5$
ECPO		Strategy = 1, archSize = 30 and NPI = 2
MECPO		Strategy = 1, archSize = 30, NPI = 2, $C_1 = 3$, $C_2 = 0.25$, and $\beta = \text{random number}$

4.3. Statistical Results

The mean and STD of the optimum value acquired by the MECPO method and the counterparts are reported in Table 3 for each CEC'17 function; the optimal results are highlighted in boldface. The obtained results proved that the MECPO technique is achieved the best values in solving 21 of CEC'17 functions. Moreover, MECPO gained the first rank.

Table 3. The mean and STD of optimal values of the OF for thirty trials achieved with the various techniques on the CEC'17 benchmark with dimension = 30.

#	Measure	GSA	GWO	WOA	SCA	EO	HHO	EPPO	MECPO
1	Mean	7.46×10^7	1.99×10^9	1.08×10^9	1.84×10^{10}	6.40×10^3	3.17×10^7	7.14×10^8	3.78×10^3
	STD	1.57×10^8	1.30×10^9	3.15×10^8	3.07×10^9	6.54×10^3	7.47×10^6	1.31×10^9	4.94×10^3
3	Mean	9.62×10^4	5.33×10^4	2.95×10^5	6.66×10^4	2.69×10^4	3.99×10^4	2.23×10^4	1.06×10^5
	STD	1.10×10^4	1.32×10^4	7.46×10^4	1.33×10^4	8.38×10^3	6.79×10^3	2.29×10^4	2.52×10^4
4	Mean	6.54×10^2	5.96×10^2	8.74×10^2	2.35×10^3	4.99×10^2	5.55×10^2	5.18×10^2	4.90×10^2
	STD	1.25×10^2	5.81×10^1	4.64×10^1	6.92×10^2	2.48×10^1	1.46×10^1	4.36×10^1	3.48×10^1
5	Mean	7.39×10^2	6.16×10^2	8.58×10^2	8.14×10^2	6.77×10^2	7.40×10^2	6.16×10^2	5.55×10^2
	STD	2.43×10^1	2.30×10^1	5.22×10^1	2.64×10^1	2.44×10^1	4.90×10^1	2.55×10^1	5.50×10^1
6	Mean	6.58×10^2	6.11×10^2	6.91×10^2	6.60×10^2	6.01×10^2	6.73×10^2	6.19×10^2	6.00×10^2
	STD	3.99	4.34	1.52×10^1	6.28	8.31×10^{-1}	9.36	6.71	1.88×10^{-1}
7	Mean	9.62×10^2	8.86×10^2	1.29×10^3	1.21×10^3	8.40×10^2	1.30×10^3	9.68×10^2	8.40×10^2
	STD	5.50×10^1	5.02×10^1	5.18×10^1	4.61×10^1	3.33×10^1	5.43×10^1	7.65×10^1	6.25×10^1
8	Mean	9.63×10^2	8.96×10^2	1.07×10^3	1.09×10^3	8.86×10^2	9.68×10^2	9.01×10^2	8.35×10^2
	STD	1.64×10^1	1.56×10^1	4.81×10^1	2.13×10^1	1.81×10^1	3.46×10^1	2.20×10^1	2.73×10^1
9	Mean	4.17×10^3	2.26×10^3	1.16×10^4	7.92×10^3	1.26×10^3	7.55×10^3	2.28×10^3	9.48×10^2
	STD	4.17×10^2	6.75×10^2	5.87×10^3	1.54×10^3	4.48×10^2	1.90×10^3	1.01×10^3	4.73×10^1
10	Mean	5.39×10^3	4.80×10^3	6.73×10^3	8.66×10^3	5.21×10^3	6.14×10^3	4.68×10^3	8.04×10^3
	STD	4.92×10^2	1.15×10^3	9.07×10^2	3.33×10^2	7.53×10^2	3.57×10^2	7.77×10^2	5.16×10^2
11	Mean	3.97×10^3	2.04×10^3	6.90×10^3	3.45×10^3	1.29×10^3	1.29×10^3	4.04×10^1	1.17×10^3
	STD	1.12×10^3	8.34×10^2	3.18×10^3	1.08×10^3	4.29×10^1	3.41×10^1	7.49×10^2	1.68×10^3

Table 3. Cont.

#	Measure	GSA	GWO	WOA	SCA	EO	HHO	EPCO	MEPCO
12	Mean	1.25×10^8	1.34×10^8	3.17×10^8	2.15×10^9	7.58×10^5	3.69×10^7	2.99×10^6	1.23×10^6
	STD	1.29×10^8	2.48×10^8	1.29×10^8	5.75×10^8	7.77×10^5	2.63×10^7	3.71×10^6	6.53×10^5
13	Mean	3.40×10^4	3.51×10^5	1.21×10^6	9.15×10^8	1.79×10^4	6.68×10^5	2.16×10^5	1.39×10^4
	STD	9.35×10^3	6.03×10^5	3.84×10^5	4.21×10^8	1.68×10^4	4.26×10^5	8.31×10^5	1.37×10^4
14	Mean	1.03×10^6	5.06×10^5	3.17×10^6	4.70×10^5	5.14×10^4	4.12×10^5	1.19×10^5	9.76×10^4
	STD	3.52×10^5	4.37×10^5	2.59×10^6	3.85×10^5	3.70×10^4	2.54×10^5	4.22×10^5	8.76×10^4
15	Mean	1.78×10^4	5.95×10^5	2.27×10^6	4.26×10^7	6.10×10^3	1.11×10^5	1.08×10^4	6.10×10^3
	STD	5.93×10^3	1.23×10^6	3.67×10^6	3.22×10^7	5.89×10^3	1.13×10^5	9.09×10^3	5.50×10^3
16	Mean	3.47×10^3	2.53×10^3	4.06×10^3	3.95×10^3	2.41×10^3	3.23×10^3	2.65×10^3	2.57×10^3
	STD	3.34×10^2	2.52×10^2	1.09×10^3	2.38×10^2	3.42×10^2	2.66×10^2	2.89×10^2	5.61×10^2
17	Mean	2.88×10^3	2.07×10^3	2.91×10^3	2.64×10^3	2.12×10^3	2.50×10^3	2.26×10^3	1.93×10^3
	STD	2.44×10^2	2.00×10^2	3.23×10^2	2.88×10^2	2.19×10^2	3.09×10^2	2.51×10^2	2.20×10^2
18	Mean	5.16×10^5	2.43×10^6	1.24×10^7	9.49×10^6	7.54×10^5	2.54×10^6	1.95×10^5	1.88×10^6
	STD	4.03×10^5	5.15×10^6	6.47×10^6	4.99×10^6	5.47×10^5	1.02×10^6	2.42×10^5	2.75×10^6
19	Mean	1.35×10^5	3.06×10^6	6.09×10^6	7.10×10^7	5.99×10^3	8.94×10^5	1.19×10^4	9.67×10^3
	STD	1.08×10^5	8.77×10^6	5.06×10^6	4.12×10^7	2.03×10^3	5.59×10^5	1.16×10^4	1.15×10^4
20	Mean	3.07×10^3	2.45×10^3	2.82×10^3	2.90×10^3	2.29×10^3	2.85×10^3	2.49×10^3	2.21×10^3
	STD	2.66×10^2	1.73×10^2	1.98×10^2	1.43×10^2	1.26×10^2	1.86×10^2	2.40×10^2	1.85×10^2
21	Mean	2.62×10^3	2.40×10^3	2.60×10^3	2.59×10^3	2.437×10^3	2.61×10^3	2.40×10^3	2.36×10^3
	STD	3.59×10^1	2.46×10^1	2.00×10^1	2.62×10^1	2.02×10^1	4.52×10^1	2.44×10^1	5.82×10^1
22	Mean	7.25×10^3	4.99×10^3	6.55×10^3	9.01×10^3	3.51×10^3	5.77×10^3	4.53×10^3	7.79×10^3
	STD	5.08×10^2	1.84×10^3	2.45×10^3	2.49×10^3	1.97×10^3	2.99×10^3	1.88×10^3	3.09×10^3
23	Mean	3.80×10^3	2.80×10^3	3.07×10^3	3.05×10^3	2.73×10^3	3.25×10^3	2.81×10^3	2.68×10^3
	STD	1.85×10^2	6.09×10^1	1.06×10^2	2.96×10^1	1.92×10^1	6.49×10^1	4.82×10^1	8.28
24	Mean	3.44×10^3	2.94×10^3	3.23×10^3	3.24×10^3	2.99×10^3	3.43×10^3	2.96×10^3	3.00×10^3
	STD	1.32×10^2	5.36×10^1	6.98×10^1	3.01×10^1	2.34×10^1	1.17×10^2	3.88×10^1	1.47×10^1
25	Mean	2.99×10^3	3.01×10^3	3.10×10^3	3.48×10^3	2.95×10^3	2.94×10^3	2.93×10^3	2.89×10^3
	STD	2.57×10^1	4.51×10^1	3.28×10^1	1.43×10^2	2.73	1.62×10^1	3.42×10^1	1.27×10^1
26	Mean	7.85×10^3	4.90×10^3	9.31×10^3	7.60×10^3	5.87×10^3	8.21×10^3	5.21×10^3	4.08×10^3
	STD	6.30×10^2	3.12×10^2	1.01×10^3	3.93×10^2	7.24×10^2	1.18×10^3	8.11×10^2	1.79×10^2
27	Mean	5.10×10^3	3.25×10^3	3.48×10^3	3.51×10^3	3.22×10^3	3.65×10^3	3.27×10^3	3.22×10^3
	STD	4.19×10^2	1.78×10^1	8.82×10^1	4.41×10^1	9.77	3.28×10^2	3.14×10^1	1.33×10^1
28	Mean	3.56×10^3	3.51×10^3	3.56×10^3	4.23×10^3	3.22×10^3	3.35×10^3	3.30×10^3	3.23×10^3
	STD	2.08×10^2	1.98×10^2	1.50×10^2	2.36×10^2	1.93×10^1	3.48×10^1	8.87×10^1	2.34×10^1
29	Mean	5.28×10^3	3.95×10^3	5.42×10^3	5.05×10^3	3.68×10^3	4.90×10^3	3.94×10^3	3.46×10^3
	STD	3.33×10^2	1.80×10^2	3.70×10^2	1.93×10^2	2.27×10^2	6.31×10^2	2.23×10^2	1.43×10^2
30	Mean	3.18×10^6	9.29×10^6	3.98×10^7	1.41×10^8	9.95×10^3	7.82×10^6	2.52×10^4	9.01×10^3
	STD	4.09×10^6	8.10×10^6	3.06×10^7	4.86×10^7	3.45×10^3	3.85×10^6	5.26×10^4	2.89×10^3

The optimal values obtained are in bold.

4.4. Convergence Analysis

The convergence characteristics curves analysis of the MECPO technique and the other recent techniques over the CEC'17 functions are illustrated in Figure 5. It is clear from the charts that the proposed MECPO reached a stable point; therefore, it reaches the lowest average of the best so-far solutions on all functions. The achieved fast convergence qualifies the proposed MECPO to be in the first rank and solves problems that require fast computation.

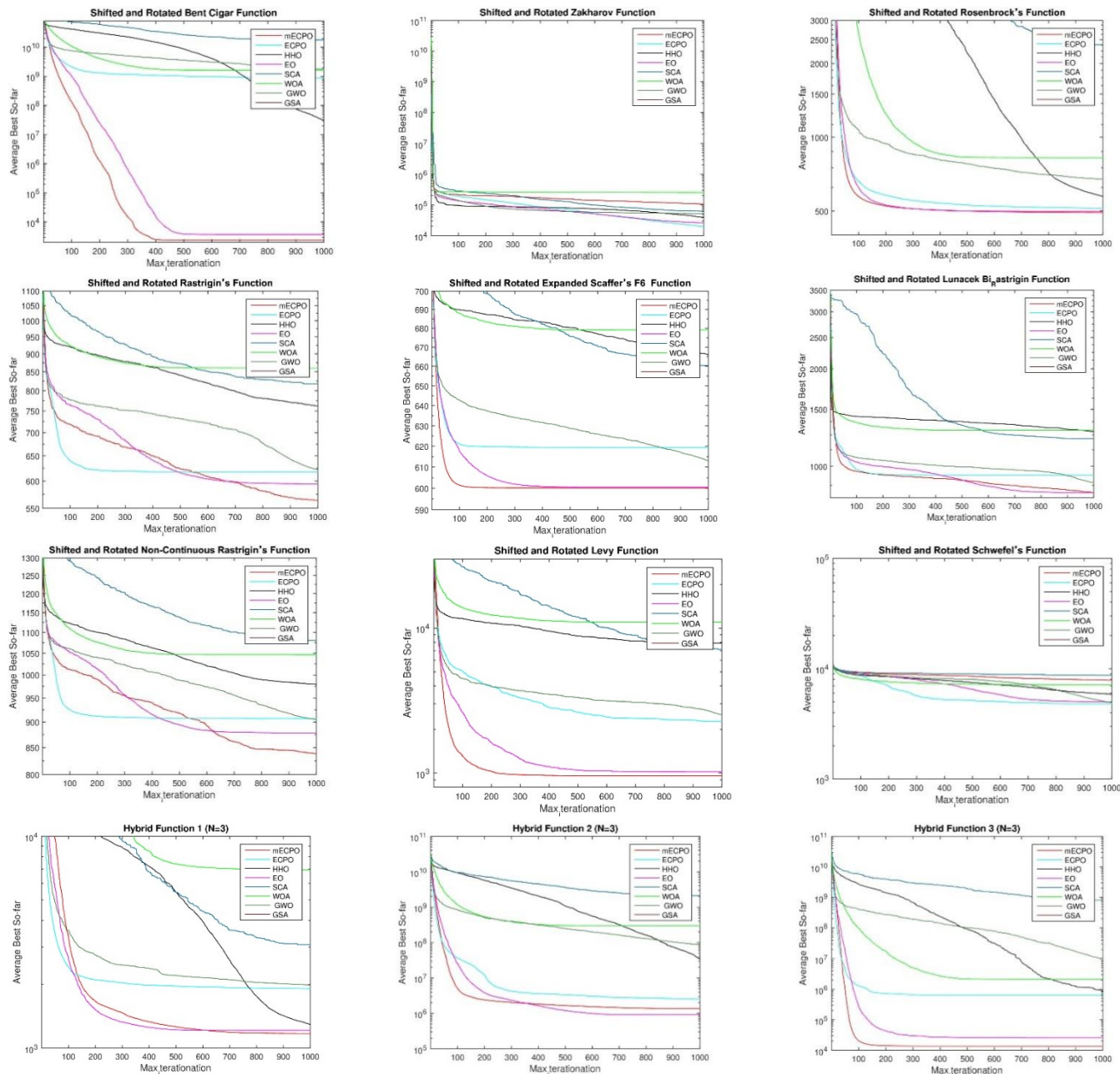


Figure 5. Cont.

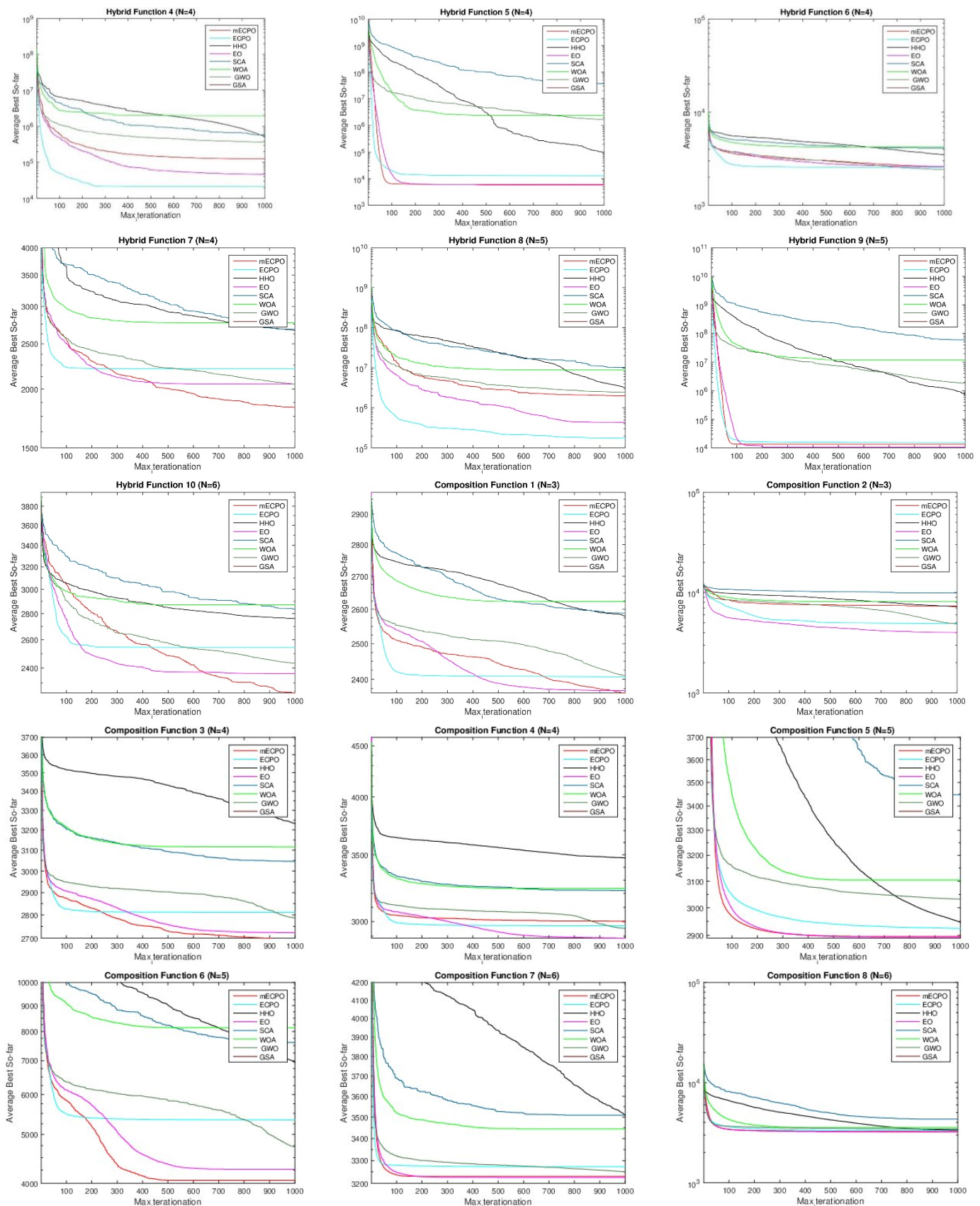


Figure 5. Cont.

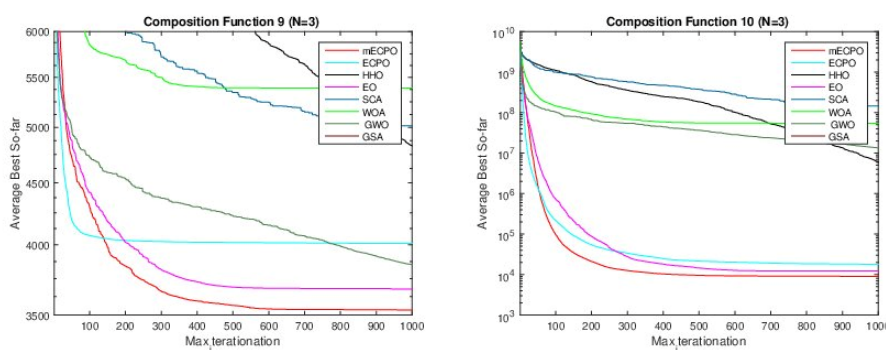


Figure 5. The convergence curves of the MECPO and the counterparts achieved on CEC'17 functions with Dim = 30.

4.5. Boxplot's Analysis

Hence, the CEC'17 test suite has many local optima, so to know the distribution of best fitness, the boxplot analysis is drawn to describe data distributions into quartiles for each technique and each function in Figure 6. The box plots of the MECPO technique are very narrow for most functions compared to various recent methods distributions and, therefore, with the best values. In fact, the MECPO technique performs better than the other methods in most test functions.

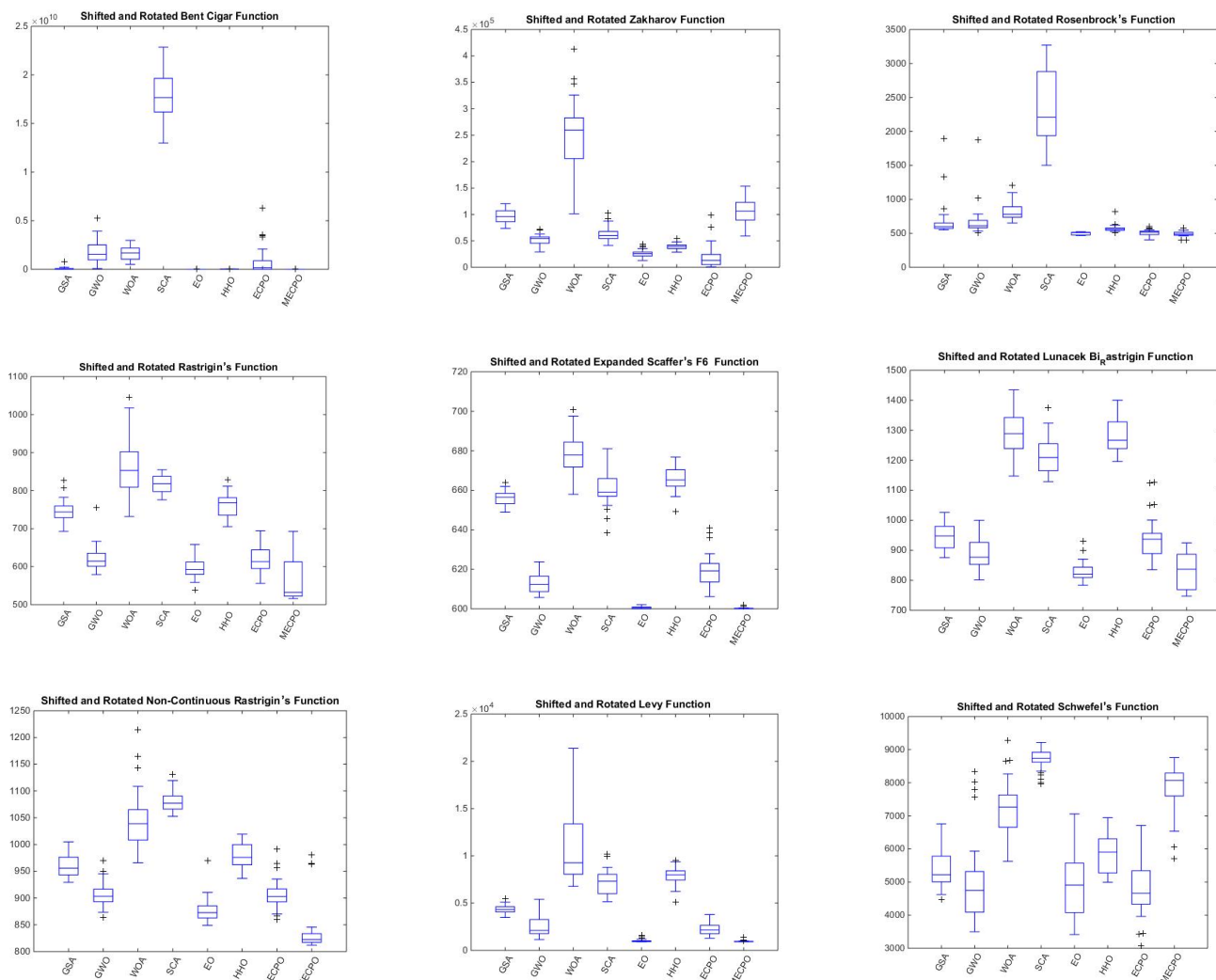
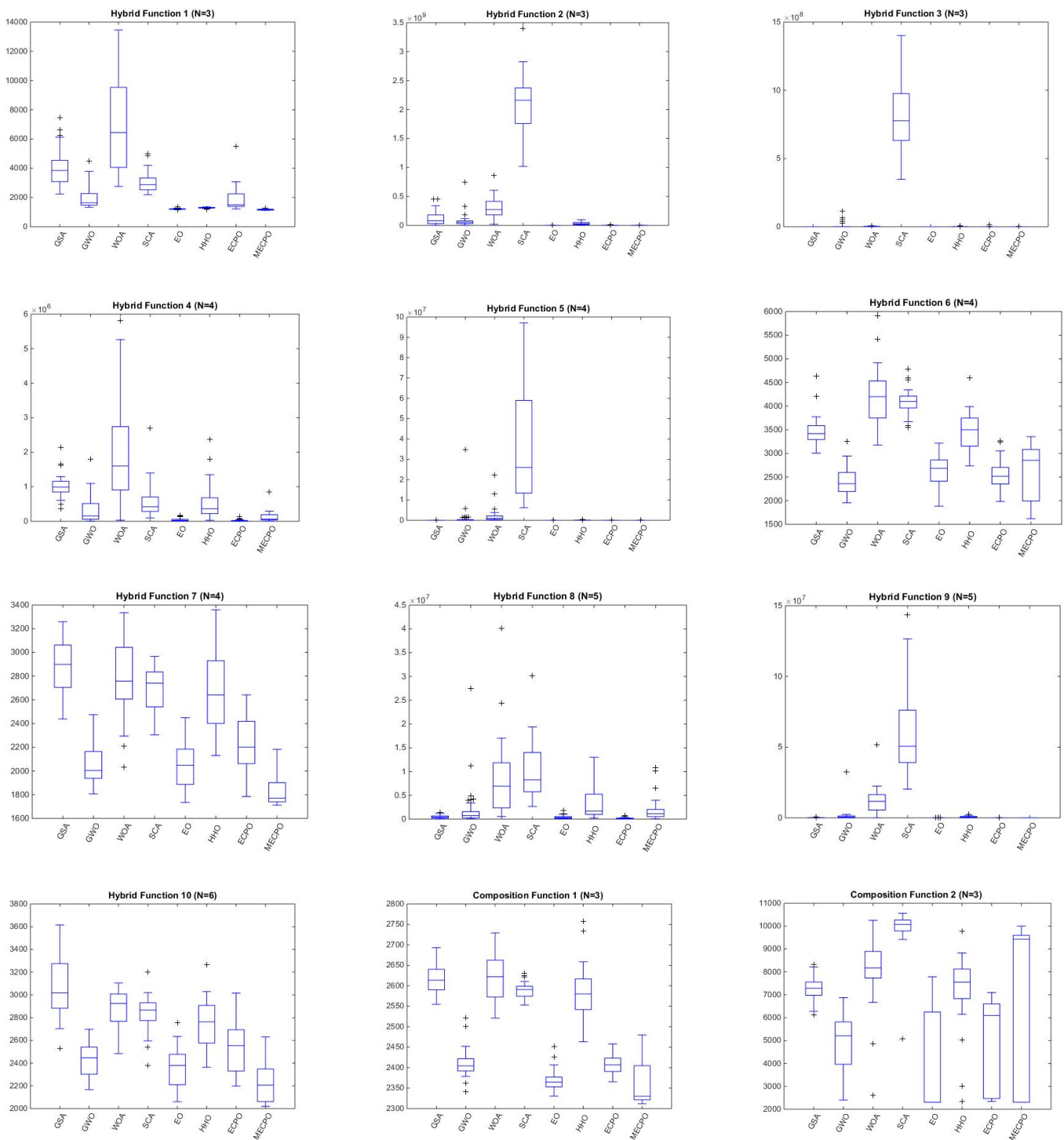


Figure 6. Cont.

**Figure 6. Cont.**

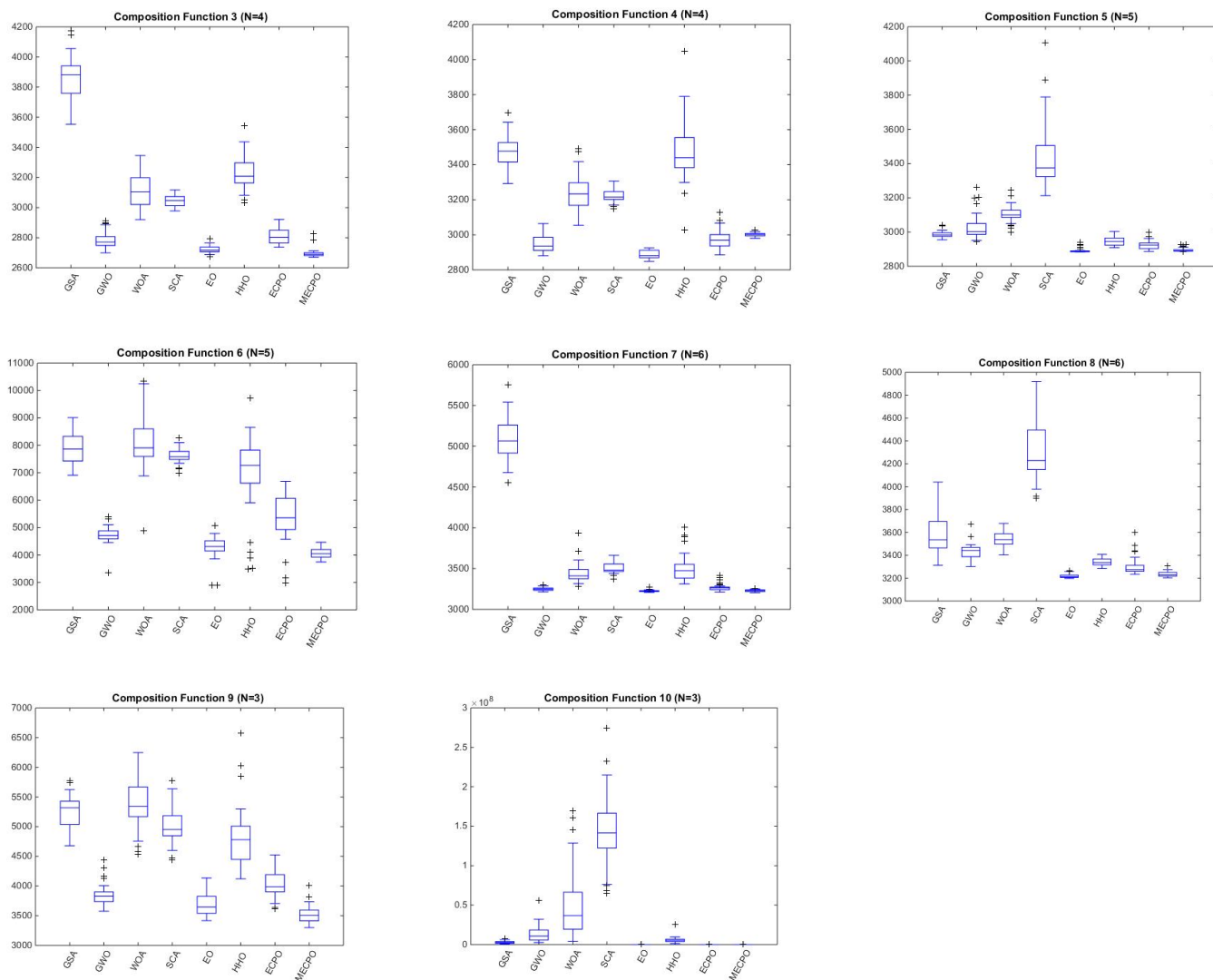


Figure 6. The boxplot curves of the MECPO technique and the other techniques achieved for CEC'17 functions with dimension = 30.

4.6. The Wilcoxon Signed-Rank Test

Although metaheuristics are stochastic methods, the predicted performance should be more accurate. To verify the obtained statistical results and evaluate the significance, Wilcoxon's rank-sum test was performed. More details about Wilcoxon's test are given in [49]. The average pair-wise comparison of the optimal solutions with a significance level equal to 5% is reported in Table 4. In the same context, the results are statistically significant for all CEC'17 functions for most functions. The obtained results in Table 4 reveal that the performance of MECPO is superior over the other counterparts.

Table 4. Results of Wilcoxon’s test ($p \geq 0.05$) between the MECPO technique and the various recent techniques for the CEC’17 functions with Dim = 30.

#	GSA vs. MECPO	GWO vs. MECPO	WOA vs. MECPO	SCA vs. MECPO	EO vs. MECPO	HHO vs. MECPO	EPCO vs. MECPO
1	0.0030	3.0199×10^{-11}	3.0199×10^{-11}	3.0199×10^{-11}	0.2226	3.0199×10^{-11}	8.9934×10^{-11}
3	0.0748	7.3891×10^{-11}	5.0723×10^{-10}	8.4848×10^{-9}	3.0199×10^{-11}	3.0199×10^{-11}	1.4643×10^{-10}
4	6.6955×10^{-11}	4.1997×10^{-10}	3.0199×10^{-11}	3.0199×10^{-11}	0.5011	3.1967×10^{-9}	0.0251
5	3.0199×10^{-11}	4.2175×10^{-4}	3.0199×10^{-11}	3.0199×10^{-11}	0.0025	3.0199×10^{-11}	4.2175×10^{-4}
6	3.0199×10^{-11}	3.0199×10^{-11}	3.0199×10^{-11}	3.0199×10^{-11}	0.0013	3.0199×10^{-11}	3.0199×10^{-11}
7	3.4971×10^{-9}	0.0017	3.0199×10^{-11}	3.0199×10^{-11}	0.8883	3.0199×10^{-11}	6.0459×10^{-7}
8	7.7725×10^{-9}	9.0632×10^{-8}	4.5043×10^{-11}	3.0199×10^{-11}	9.0632×10^{-8}	8.8910×10^{-10}	7.6950×10^{-8}
9	3.0199×10^{-11}	3.6897×10^{-11}	3.0199×10^{-11}	3.0199×10^{-11}	0.2519	3.0199×10^{-11}	3.3384×10^{-11}
10	1.6132×10^{-10}	6.5183×10^{-9}	8.1200×10^{-4}	9.8329×10^{-8}	1.2057×10^{-10}	8.1014×10^{-10}	8.1527×10^{-11}
11	3.0199×10^{-11}	3.0199×10^{-11}	3.0199×10^{-11}	3.0199×10^{-11}	6.9125×10^{-4}	1.6132×10^{-10}	6.6955×10^{-11}
12	2.1544×10^{-10}	6.0658×10^{-11}	3.0199×10^{-11}	3.0199×10^{-11}	0.1120	3.0199×10^{-11}	0.0339
13	4.3106×10^{-8}	3.6897×10^{-11}	3.0199×10^{-11}	3.0199×10^{-11}	0.0292	3.0199×10^{-11}	0.0850
14	6.6955×10^{-11}	0.0191	7.7725×10^{-9}	2.3897×10^{-8}	0.0030	2.6784×10^{-6}	8.8411×10^{-7}
15	1.3111×10^{-8}	8.9934×10^{-11}	3.0199×10^{-11}	3.0199×10^{-11}	0.8073	3.6897×10^{-11}	0.0117
16	3.4971×10^{-9}	0.1907	6.0658×10^{-11}	3.0199×10^{-11}	0.5895	2.0283×10^{-7}	0.5493
17	3.0199×10^{-11}	6.0459×10^{-7}	4.0772×10^{-11}	3.0199×10^{-11}	5.8587×10^{-6}	4.0772×10^{-11}	2.1947×10^{-8}
18	2.8389×10^{-4}	0.3183	3.5708×10^{-6}	2.9215×10^{-9}	6.3560×10^{-5}	0.0501	2.1947×10^{-8}
19	6.6955×10^{-11}	8.1014×10^{-10}	3.0199×10^{-11}	3.0199×10^{-11}	0.1809	3.0199×10^{-11}	0.7731
20	4.0772×10^{-11}	5.9706×10^{-5}	6.0658×10^{-11}	9.9186×10^{-11}	0.0080	9.7555×10^{-10}	1.6062×10^{-6}
21	3.0199×10^{-11}	6.9125×10^{-4}	3.0199×10^{-11}	3.0199×10^{-11}	0.0176	4.9752×10^{-11}	0.0014
22	0.0080	0.0080	0.1580	5.5329×10^{-8}	5.8737×10^{-4}	0.0170	0.0080
23	3.0199×10^{-11}	2.6695×10^{-9}	3.0199×10^{-11}	3.0199×10^{-11}	2.1540×10^{-6}	3.0199×10^{-11}	5.5727×10^{-10}
24	3.0199×10^{-11}	1.7836×10^{-4}	3.0199×10^{-11}	3.0199×10^{-11}	3.0199×10^{-11}	3.3384×10^{-11}	6.2027×10^{-4}
25	3.0199×10^{-11}	3.0199×10^{-11}	3.0199×10^{-11}	3.0199×10^{-11}	0.0519	9.7555×10^{-10}	2.1540×10^{-6}
26	3.0199×10^{-11}	6.1210×10^{-10}	3.0199×10^{-11}	3.0199×10^{-11}	4.4592×10^{-4}	1.8731×10^{-7}	1.0666×10^{-7}
27	3.0199×10^{-11}	1.1058×10^{-4}	3.0199×10^{-11}	3.0199×10^{-11}	0.1453	3.0199×10^{-11}	1.2860×10^{-6}
28	3.0199×10^{-11}	3.3384×10^{-11}	3.0199×10^{-11}	3.0199×10^{-11}	0.0053	5.4941×10^{-11}	8.3520×10^{-8}
29	3.0199×10^{-11}	1.8500×10^{-8}	3.0199×10^{-11}	3.0199×10^{-11}	0.0018	3.0199×10^{-11}	8.1014×10^{-10}
30	3.0199×10^{-11}	3.0199×10^{-11}	3.0199×10^{-11}	3.0199×10^{-11}	0.0315	3.0199×10^{-11}	6.2828×10^{-6}

5. The Results and Discussion of Real-World Application

The numerical simulation of the proposed MECPO algorithm for identifying parameters of SDM, DDM, and TDM is illustrated in this section. Figure 7 displays the estimation process for the PV models and their validation procedure. The seven recent techniques COOT, EO, GPC, and MPA, as well as the conventional ECPO, are used in the comparison. Table 5 presents the parameter settings of the selected algorithms. All mentioned techniques have been executed for 20 independent runs using MATLAB 2016a platform with an Intel® core TM i5-4210U CPU, 1.70 GHz, 8 GB RAM Laptop.

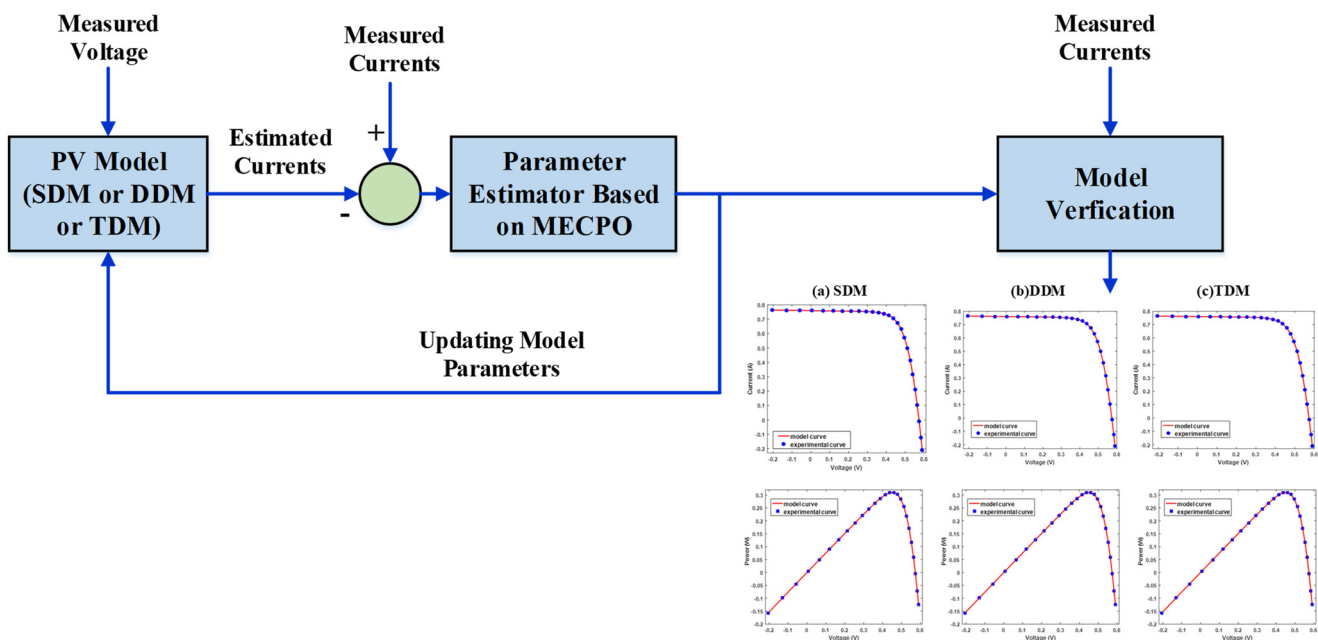


Figure 7. Global parameter estimation representation based on MECPO optimization algorithm.

Table 5. Parameter settings of the selected techniques.

Algorithms	Parameters Setting
Common settings	Population size: $nPop = 100$ for SDM and $nPop = 200$ for DDM and TDM Maximum iterations: $Max_iter = 1000$ Number of independent runs: 20
GPC	$G = 9.8$, $Teta = 14$, $MuMin = 1$, $MuMax = 10$, $pSS = 0.5$
EO	$a_1 = 2$, $a_2 = 1$
MPA	$FADs = 0.2$, $P = 0.5$, $C = 0.05$, $e = 0.25$

5.1. Case 1: Single-Diode Model (SDM)

In the first case, Table 6 tabulated the optimal parameter values and the fitness values obtained by the MECPO algorithm, original ECPO, and four well-known algorithms for the SDM. The convergence characteristics for all techniques are displayed in Figure 8. The value of the parameters in the case of the SDM achieved using the five algorithms are presented in Table 6. Moreover, Figure 9 presents the boxplot of COOT, ECPO, EO, GPC, MPA, and the proposed MECPO techniques for the single diode, which illustrates the distribution of results achieved by various techniques in 20 trials. Table 6 tabulates the measured data's voltage and current values and the simulated current value, simulated power value, relative error, and absolute error using the proposed MECPO for SDM.

Table 6. Calculated parameter in case of the SDM obtained by the proposed algorithm and other recent techniques.

Algorithm	MECPO	ECPO	COOT	GPC	EO	MPA
$R_s (\Omega)$	0.036377	0.151767	0.033574	0.000748	0.027151	0.038619
$R_{sh}(\Omega)$	53.71852	35.53006	100	17.97128	99.52477	40.87662
I_{ph} (A)	0.760776	0.677648	0.760476	0.776792	0.761999	0.761135
I_{sd} (A)	3.23×10^{-7}	0.000155	6.57×10^{-7}	1.87×10^{-5}	2.07×10^{-6}	1.79×10^{-7}
n	1.215672	1.984596	1.277162	1.684806	1.39214	1.168594
RMSE	9.86×10^{-4}	0.717356	0.001731	0.018806	0.004147	0.00149

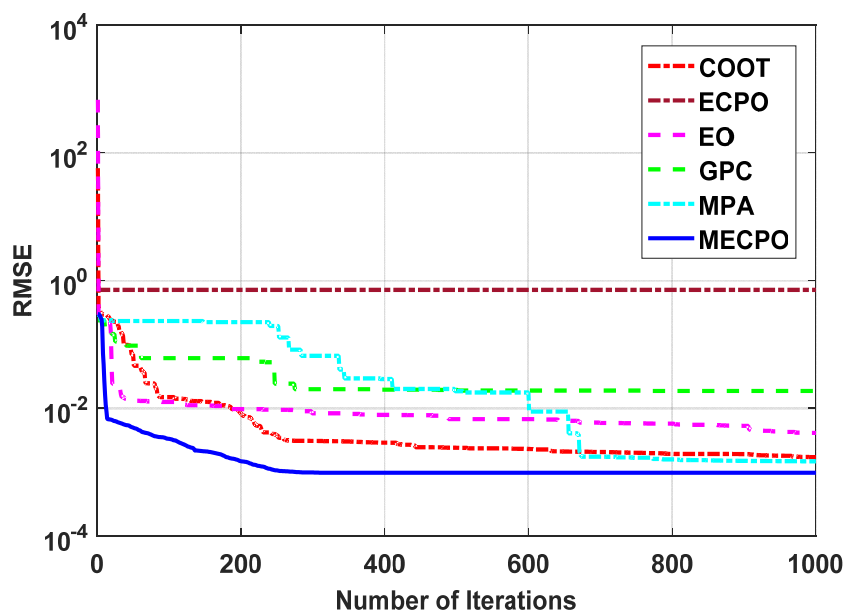


Figure 8. Convergence curve of the MECPO and other recent algorithms for the SDM.

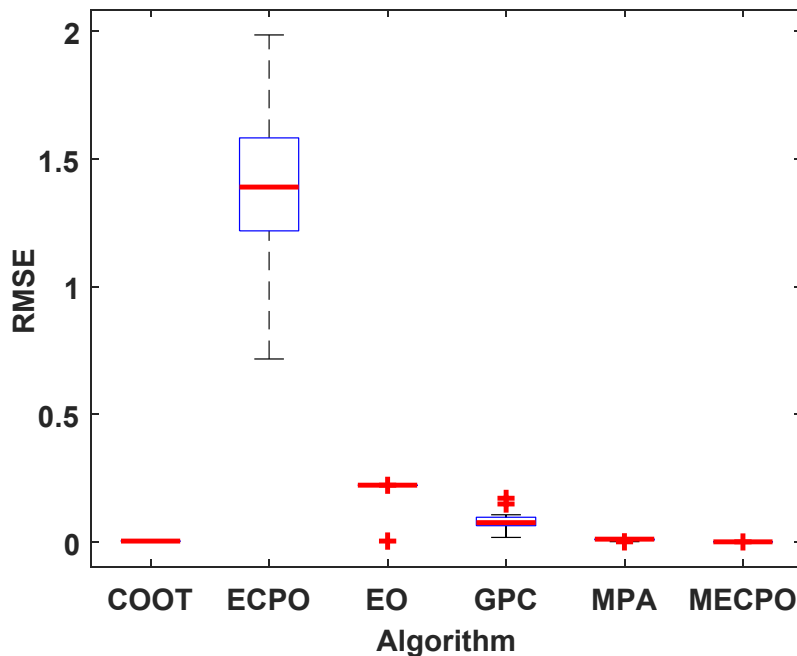


Figure 9. Best RMSE boxplot in 20 runs of the MECPO and other recent algorithms for the SDM.

In Table 7, the fitness value (9.86×10^{-4}) obtained by the proposed MECPO technique is less than any other algorithm. As shown in Figure 8, The MECPO algorithm has a high convergence speed compared with the other recent algorithms from the initial search stage to the end of iterations, and this confirms the high precision of the proposed algorithm. The five metrics results after 20 independent runs of all algorithms in Table 7 indicate that the effectiveness and robustness of the proposed algorithm are better than other techniques.

Table 7. Statistical results of the proposed MECPO algorithm and other recent algorithms in the case of the SDM.

Algorithm	Best	Mean	Median	Worst	STD
MECPO	0.000986	0.000986	0.000986	0.000986	2.31×10^{-16}
ECPO	0.717356	1.395899	1.390179	1.985481	0.316597
COOT	0.001731	0.004135	0.004434	0.005851	0.001238
GPC	0.018806	0.081121	0.076739	0.171743	0.035797
EO	0.004147	0.211926	0.222861	0.222861	0.048906
MPA	0.00149	0.009937	0.011736	0.012607	0.003505

The optimal values obtained are in bold.

According to the comparisons on the solution distribution in Figure 9, it can be seen that the MECPO technique gives the best performance compared with the other techniques in terms of precision and strength. As can be seen from Table 8, the calculated data of the SDM obtained by the proposed MECPO technique are compatible with the measured data.

Table 8. Measured and simulated data of voltages, currents, and power and the absolute errors values using MECPO for SDM.

Rank	Experimental Data			Simulated Current Data		Simulated Power Data	
	V (V)	I (A)	P (W)	I_{sim} (A)	IAE_I (A)	P_{sim} (W)	$IAEP$ (W)
1	-0.2057	0.764	-0.157155	0.76409	8.80×10^{-5}	-0.15717	2.00×10^{-5}
2	-0.1291	0.762	-0.098374	0.76266	6.63×10^{-4}	-0.09846	9.00×10^{-5}
3	-0.0588	0.7605	-0.044717	0.76136	8.55×10^{-4}	-0.04477	5.00×10^{-5}
4	0.0057	0.7605	0.004335	0.76015	3.46×10^{-4}	0.00433	$0.00 \times 10^{+00}$
5	0.0646	0.76	0.049096	0.75906	9.45×10^{-4}	0.04903	6.00×10^{-5}
6	0.1185	0.759	0.089942	0.75804	9.58×10^{-4}	0.08983	1.10×10^{-4}
7	0.1678	0.757	0.127025	0.75709	9.20×10^{-5}	0.12704	2.00×10^{-5}
8	0.2132	0.757	0.161392	0.75614	8.59×10^{-4}	0.16121	1.80×10^{-4}
9	0.2545	0.7555	0.192275	0.75509	4.13×10^{-4}	0.19217	1.10×10^{-4}
10	0.2924	0.754	0.22047	0.75366	3.36×10^{-4}	0.22037	1.00×10^{-4}
11	0.3269	0.7505	0.245338	0.75139	8.91×10^{-4}	0.24563	2.90×10^{-4}
12	0.3585	0.7465	0.26762	0.74735	8.54×10^{-4}	0.26793	3.10×10^{-4}
13	0.3873	0.7385	0.286021	0.74012	1.62×10^{-3}	0.28665	6.30×10^{-4}
14	0.4137	0.728	0.301174	0.72738	6.18×10^{-4}	0.30092	2.60×10^{-4}
15	0.4373	0.7065	0.308952	0.70697	4.73×10^{-4}	0.30916	2.10×10^{-4}
16	0.459	0.6755	0.310055	0.67528	2.20×10^{-4}	0.30995	1.00×10^{-4}
17	0.4784	0.632	0.302349	0.63076	1.24×10^{-3}	0.30175	5.90×10^{-4}
18	0.496	0.573	0.284208	0.57193	1.07×10^{-3}	0.28368	5.30×10^{-4}
19	0.5119	0.499	0.255438	0.49961	6.07×10^{-4}	0.25575	3.10×10^{-4}
20	0.5265	0.413	0.217445	0.41365	6.49×10^{-4}	0.21779	3.40×10^{-4}
21	0.5398	0.3165	0.170847	0.31751	1.01×10^{-3}	0.17139	5.50×10^{-4}
22	0.5521	0.212	0.117045	0.21215	1.55×10^{-4}	0.11713	9.00×10^{-5}
23	0.5633	0.1035	0.058302	0.10225	1.25×10^{-3}	0.0576	7.00×10^{-4}
24	0.5736	-0.0100	-0.005736	-0.00872	1.28×10^{-3}	-0.005	7.40×10^{-4}
25	0.5833	-0.1230	-0.071746	-0.12551	2.51×10^{-3}	-0.07321	1.46×10^{-3}
26	0.59	-0.2100	-0.1239	-0.20847	1.53×10^{-3}	-0.123	9.00×10^{-4}

Figure 10 displays the individual absolute error for the current and power of the SDM using the proposed technique. Furthermore, the characteristics curve of I–V and P–V for SDM is redrawn according to the best-optimized parameters obtained by executing the proposed MECPO algorithm and presented in Figure 11. This figure confirms that our algorithm could significantly estimate the parameter values that could concretely predict the curve of experimental data.

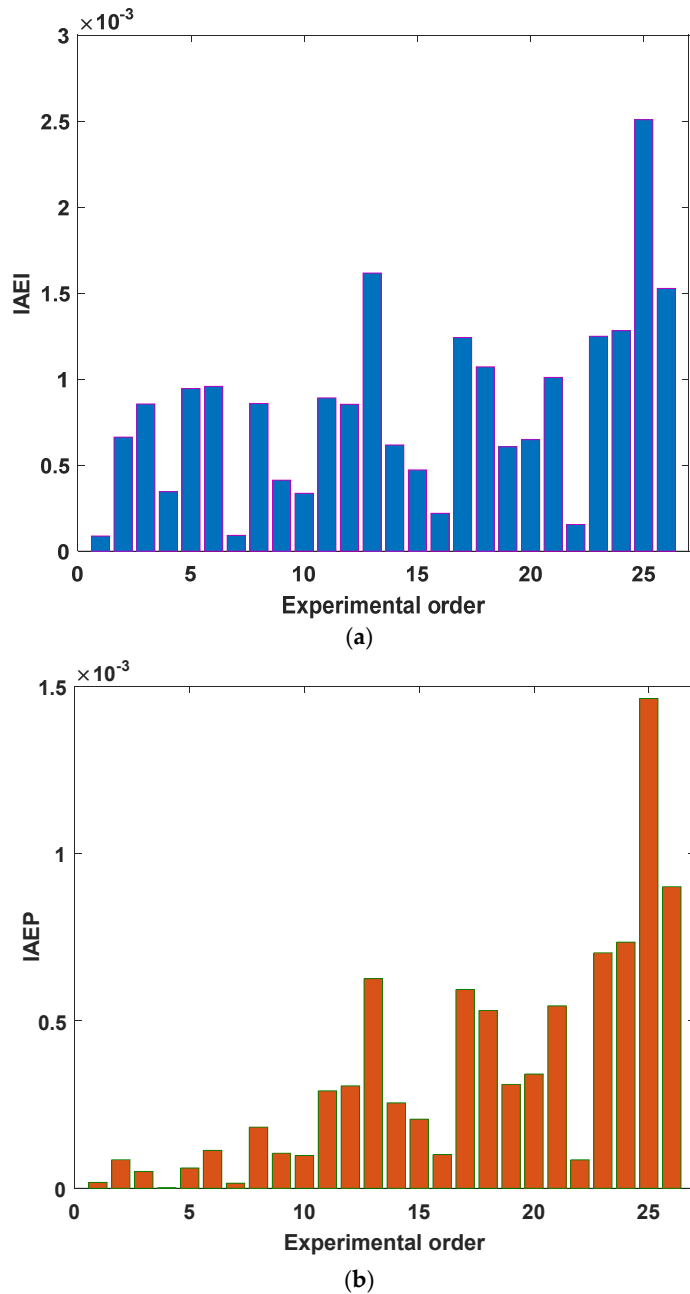


Figure 10. Individual absolute errors for current and power by the MECPO for SDM. (a) Individual absolute errors for current. (b) Individual absolute errors for power.

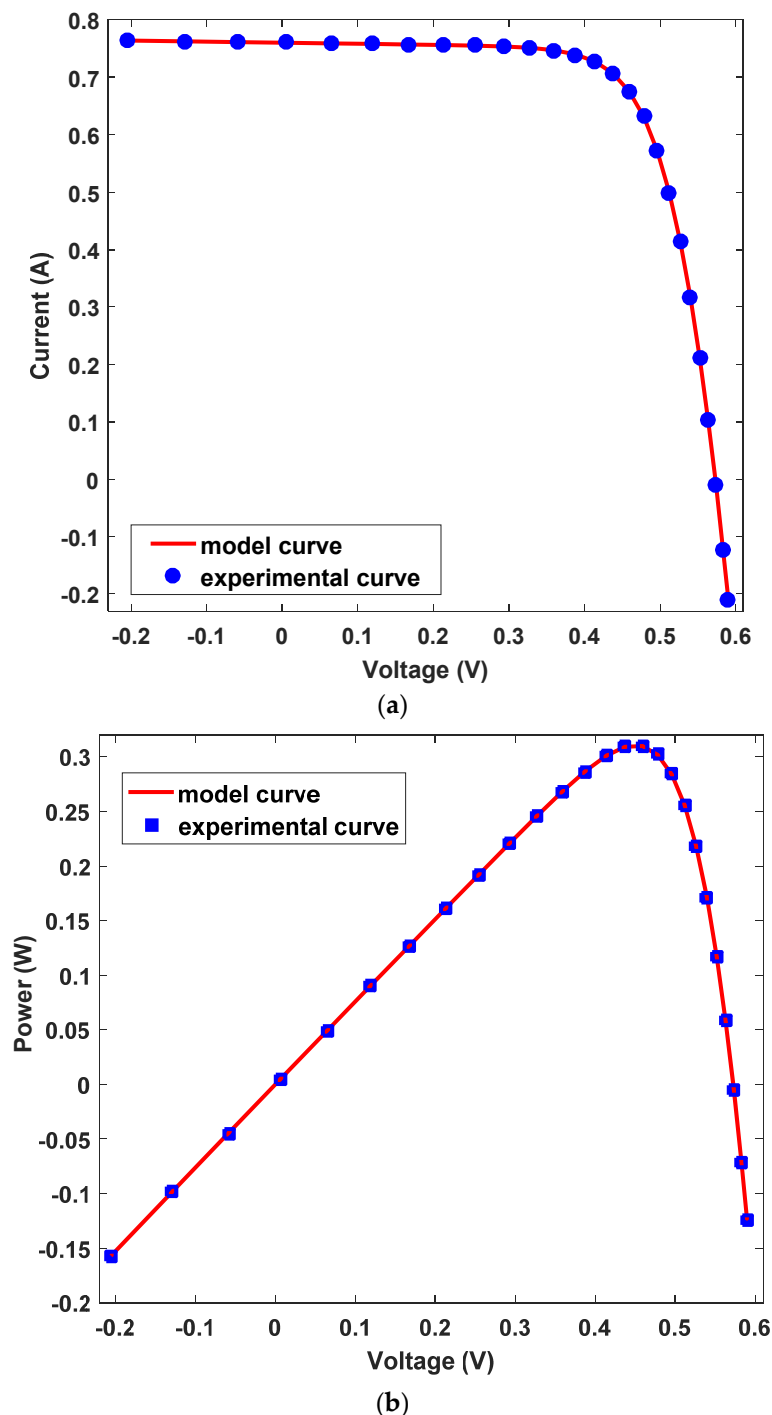


Figure 11. Comparisons between measured data and data achieved using the MECPO method for SDM (a) I-V characteristics and (b) P-V characteristics.

5.2. Case 2: Double-Diode Model (DDM)

In the second case, Table 9 presents the best values of the control variables regarding the optimal performance for the compared techniques. As shown, MECPO reaches the lowest RMSE of 0.000977 compared to the other algorithms. According to the results of the proposed MECPO algorithm, the series resistance is $0.03687\ \Omega$; shunt resistance is $57.12581\ \Omega$; the photo-generated current is 0.760789 A ; the reverse saturation currents of D1 and D2 are 3.07 and $0.231\ \mu\text{A}$, respectively; the ideality factor of the diode of D1 and D2 is 2.190954 . Figure 12 shows the convergence characteristics curves of the algorithms and

demonstrates that the capability of the MECPO technique to obtain the smallest RMSE is the fastest.

Table 9. Calculated parameter in case of the DDM obtained by the proposed algorithm and other recent techniques.

Algorithm	MECPO	ECPO	COOT	GPC	EO	MPA
$R_s (\Omega)$	0.03687	0.229884	0.0389	0.000206	0.037022	0.042933
$R_{sh}(\Omega)$	57.12581	73.68355	72.85675	100	52.11317	37.18875
I_{ph} (A)	0.760789	0.233682	0.760767	0.712533	0.76082	0.76005
I_{sd1} (A)	3.07×10^{-6}	0.433524	5.79×10^{-6}	1.28×10^{-10}	3.41×10^{-7}	2.84×10^{-19}
I_{sd2} (A)	2.31×10^{-7}	0.91553	3.76×10^{-8}	1.47×10^{-5}	1.36×10^{-9}	5.55×10^{-8}
n_1	2	1.932754	1.754744	1	1.228865	1.00292
n_2	1.190954	1.912091	1.073828	1.659771	1.000002	1.085403
RMSE	0.000977	1.515062	0.001115	0.041377	0.001001	0.003574

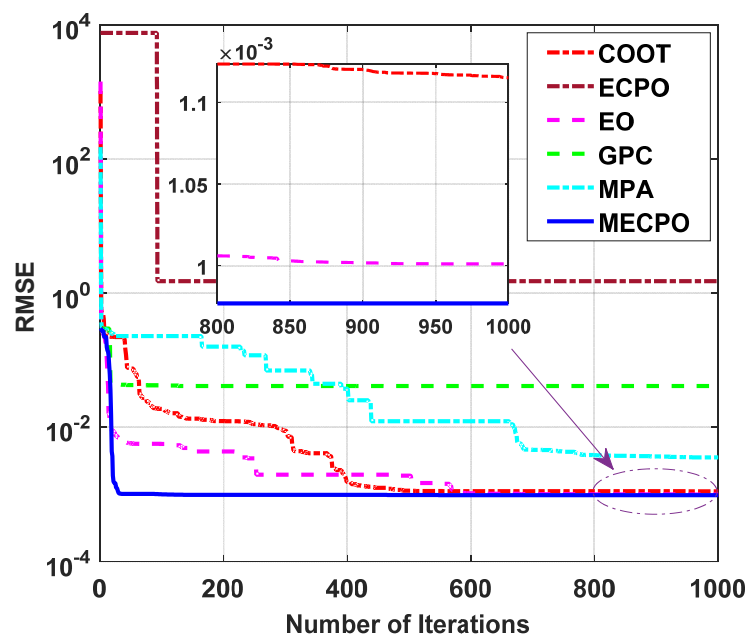


Figure 12. Convergence curve of the MECPO and other recent algorithms for the DDM.

Apparently, it is seen in Table 10 that MECPO reaches the minimum STD of 4.26×10^{-6} , which is less than ECPO, COOT, GPC, EO, and MPA that acquired STD of 0.0404779, 0.002359, 0.023745, 0.000674, and 0.002805, respectively. Figure 13 shows the box plot of the RMSE values for DDM in 20 individual runs using the MECPO and other recent algorithms.

Table 11 shows the values of measured, simulated current and the absolute errors between them (IAE_I). Furthermore, it displays the values of measured, simulated power, and the absolute errors between them (IAE_P) when applying the proposed MECPO on DDM. Moreover, Figure 14 illustrates the absolute errors of measured and simulated current and the absolute errors of experimental and simulated power using the MECPO for the DDM. Figure 15 presents the estimated parameters obtained by the proposed algorithm for the DDM that lead to the high closeness between the estimated I-V and P-V characteristics.

Table 10. Statistical results of the MECPO technique and other recent techniques in the case of the DDM.

Algorithm	Best	Mean	Median	Worst	STD
MECPO	0.000977	0.00098	0.000977	0.000989	4.26×10^{-6}
ECPO	1.515062	2.285728	2.343209	3.069671	0.404779
COOT	0.001115	0.004534	0.004441	0.009303	0.002359
GPC	0.041377	0.080475	0.072482	0.131687	0.023745
EO	0.001001	0.00141	0.001138	0.003264	0.000674
MPA	0.003574	0.011005	0.012211	0.012964	0.002805

The optimal values obtained are in bold.

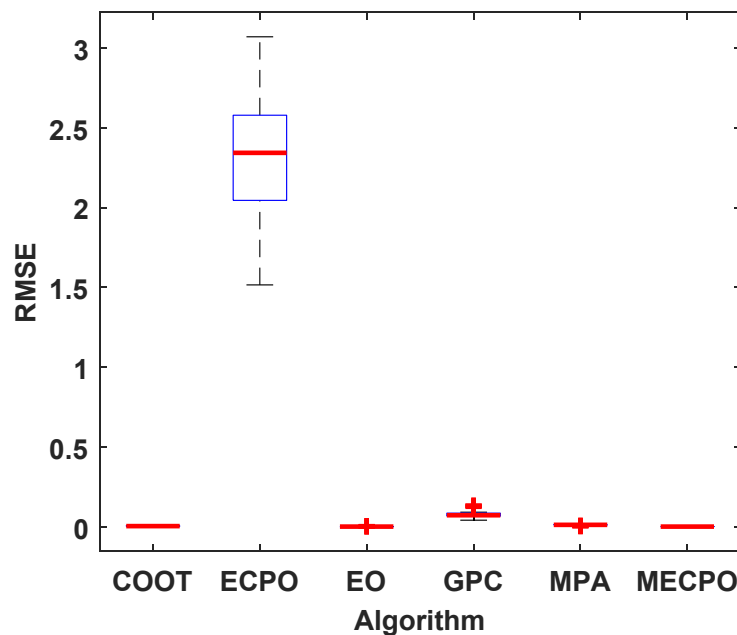


Figure 13. Best RMSE boxplot in 20 individual runs of the MECPO and other recent algorithms for the DDM.

5.3. Case 3: Triple-Diode Model (TDM)

In this case, in the case of the TDM, RMSE and the extracted nine parameters' values are displayed in Table 12. It can be clearly seen from this table that the MECPO algorithm achieves the optimal RMSE value (0.00097) among the five algorithms; further, the EO algorithm acquires the second-best RMSE value (0.001031), followed by MPA, COOT, GPC, and ECPO. Figure 16 presents the convergence curve for this case study using MECPO and other algorithms for the TDM. It is obvious that MECPO has a faster convergence rate than other techniques for single-, double-, and triple-diode models.

Table 13 gives the statistical results for the TDM. We can conclude that our algorithm can achieve the best RMSE statistical values (Min, Mean, Median, Max, and STD) in the case of the TDM compared with the other recent techniques. Moreover, to display the distribution results obtained from various algorithms, the boxplot of TDM is presented in Figure 17. It can be seen that MECPO achieves superior performance in terms of precision and robustness. The statistical results of the IAE values based on the current and power for the measured and simulated data on TDM are tabulated in Table 14. In addition, the IAEs for current and power using MECPO for TDM are displayed in Figure 18.

Table 11. Experimental and simulated data of voltages, currents, and power and the absolute errors values using MECPO for DDM.

Rank	Experimental Data			Simulated Current Data		Simulated Power Data	
	V (V)	I (A)	P (W)	I_{sim} (A)	IAE_I (A)	P_{sim} (W)	IAE_P (W)
1	-0.2057	0.764	-0.157155	0.7639	1.00×10^{-4}	-0.15713	2.10×10^{-5}
2	-0.1291	0.762	-0.098374	0.76256	5.60×10^{-4}	-0.09845	7.20×10^{-5}
3	-0.0588	0.7605	-0.044717	0.76133	8.30×10^{-4}	-0.04477	4.90×10^{-5}
4	0.0057	0.7605	0.004335	0.7602	3.00×10^{-4}	0.004333	2.00×10^{-6}
5	0.0646	0.76	0.049096	0.75916	8.40×10^{-4}	0.049041	5.50×10^{-5}
6	0.1185	0.759	0.089942	0.75819	8.10×10^{-4}	0.089845	9.60×10^{-5}
7	0.1678	0.757	0.127025	0.75726	2.60×10^{-4}	0.127069	4.40×10^{-5}
8	0.2132	0.757	0.161392	0.75632	6.80×10^{-4}	0.161246	1.46×10^{-4}
9	0.2545	0.7555	0.192275	0.75523	2.70×10^{-4}	0.192207	6.80×10^{-5}
10	0.2924	0.754	0.22047	0.75375	2.50×10^{-4}	0.220396	7.40×10^{-5}
11	0.3269	0.7505	0.245338	0.75139	8.90×10^{-4}	0.245628	2.90×10^{-4}
12	0.3585	0.7465	0.26762	0.74725	7.50×10^{-4}	0.267889	2.69×10^{-4}
13	0.3873	0.7385	0.286021	0.73993	1.43×10^{-3}	0.286576	5.55×10^{-4}
14	0.4137	0.728	0.301174	0.72716	8.40×10^{-4}	0.300827	-3.47×10^{-4}
15	0.4373	0.7065	0.308952	0.70678	2.80×10^{-4}	0.309076	1.24×10^{-4}
16	0.459	0.6755	0.310055	0.67518	3.20×10^{-4}	0.309908	1.47×10^{-4}
17	0.4784	0.632	0.302349	0.63077	1.23×10^{-3}	0.301761	5.87×10^{-4}
18	0.496	0.573	0.284208	0.57204	9.60×10^{-4}	0.283731	4.77×10^{-4}
19	0.5119	0.499	0.255438	0.49976	7.60×10^{-4}	0.255828	3.90×10^{-4}
20	0.5265	0.413	0.217445	0.41378	7.80×10^{-4}	0.217853	4.08×10^{-4}
21	0.5398	0.3165	0.170847	0.31756	1.06×10^{-3}	0.171419	5.72×10^{-4}
22	0.5521	0.212	0.117045	0.2121	1.00×10^{-4}	0.117101	5.60×10^{-5}
23	0.5633	0.1035	0.058302	0.10212	1.38×10^{-3}	0.057522	7.80×10^{-4}
24	0.5736	-0.0100	-0.005736	-0.00883	1.17×10^{-3}	-0.00507	6.70×10^{-4}
25	0.5833	-0.1230	-0.071746	-0.12556	2.56×10^{-3}	-0.07324	1.49×10^{-3}
26	0.59	-0.2100	-0.1239	-0.20832	1.68×10^{-3}	-0.12291	9.90×10^{-4}

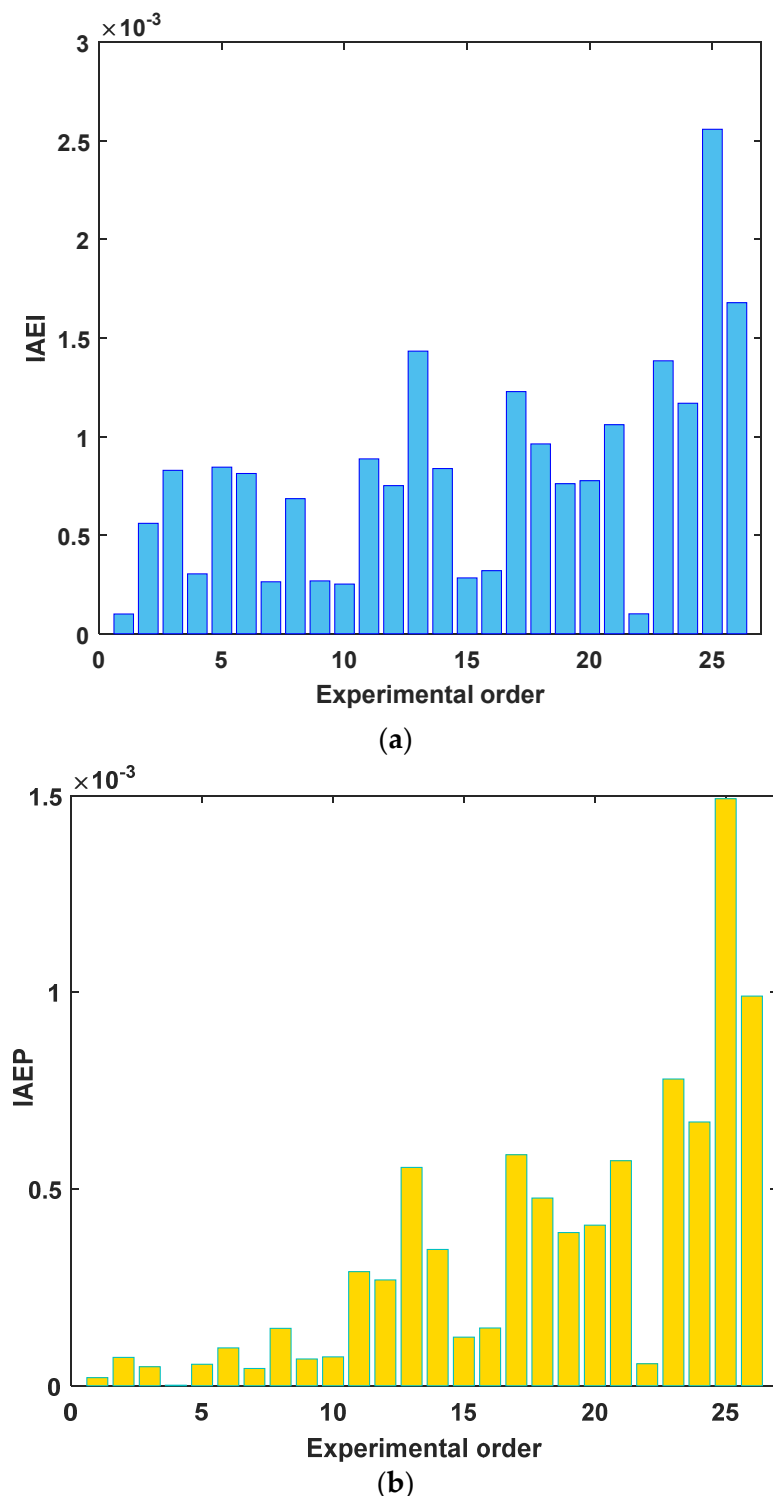


Figure 14. Individual absolute errors for current and power by the MECPO for DDM. (a) Individual absolute errors for current. (b) Individual absolute errors for power.

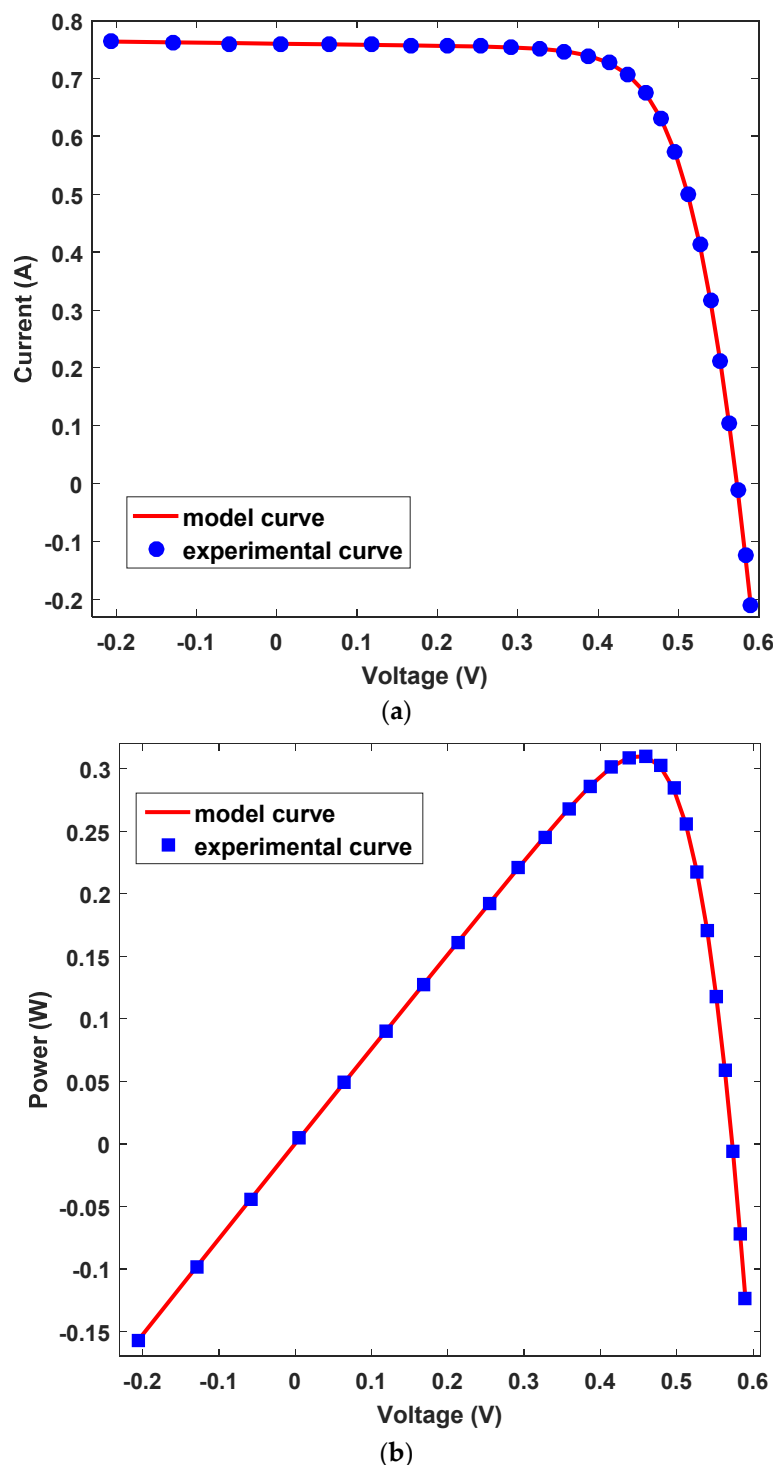
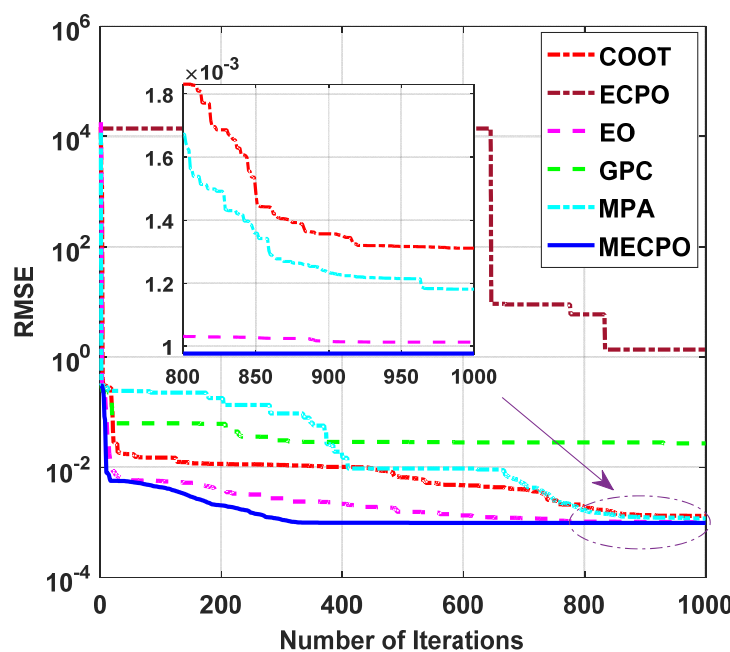


Figure 15. Comparisons between measured data and data achieved using the MECPO method for DDM (a) I-V characteristics and (b) P-V characteristics.

Table 12. Calculated parameter in case of the TDM obtained by the proposed algorithm and other recent techniques.

Algorithm	MECPO	ECPO	COOT	GPC	EO	MPA
$R_s (\Omega)$	0.03687	0.04303	0.040051	0.001854	0.037781	0.03846
$R_{sh}(\Omega)$	57.12579	100	99.89583	10.52881	54.91819	85.03041
I_{ph} (A)	0.760789	0.721768	0.760434	0.776297	0.760872	0.76019
I_{sd1} (A)	6.97×10^{-20}	0.462181	9.59×10^{-9}	1.23×10^{-5}	6.19×10^{-7}	7.53×10^{-8}
I_{sd2} (A)	3.07×10^{-6}	0.288811	5.14×10^{-6}	1×10^{-9}	8.63×10^{-9}	1.4×10^{-8}
I_{sd3} (A)	2.31×10^{-7}	0.992376	2.08×10^{-7}	1×10^{-9}	9.67×10^{-9}	1.85×10^{-6}
n_1	1.220835	2	1.000105	1.650069	1.322086	1.982829
n_2	2	1.886728	1.664525	1	1.836014	1.030268
n_3	1.190954	2	1.999564	1	1.031254	1.486103
RMSE	0.000977	1.360341	0.001311	0.027075	0.001013	0.001181

**Figure 16.** Convergence curve of the MECPO and other recent algorithms for the TDM.**Table 13.** Statistical results the MECPO technique and other recent algorithms in the case of the TDM.

Algorithm	Best	Mean	Median	Worst	STD
MECPO	0.000977	0.000979	0.000977	0.000997	5.1×10^{-6}
ECPO	1.360341	1.978315	2.019703	2.895647	0.551247
COOT	0.001311	0.004247	0.004408	0.00884	0.001786
GPC	0.027075	0.101053	0.078046	0.410851	0.085461
EO	0.001013	0.001631	0.001267	0.003046	0.000735
MPA	0.001181	0.009682	0.011312	0.012131	0.003687

The optimal values obtained are in bold.

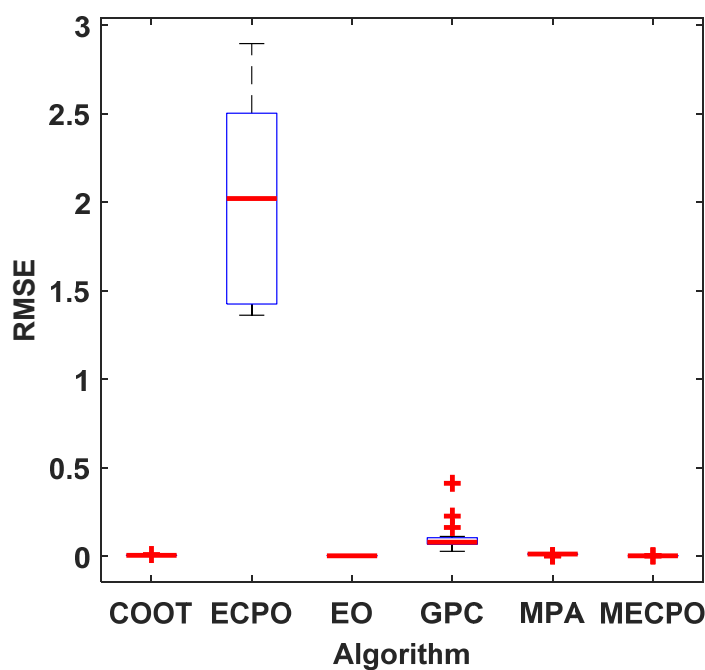


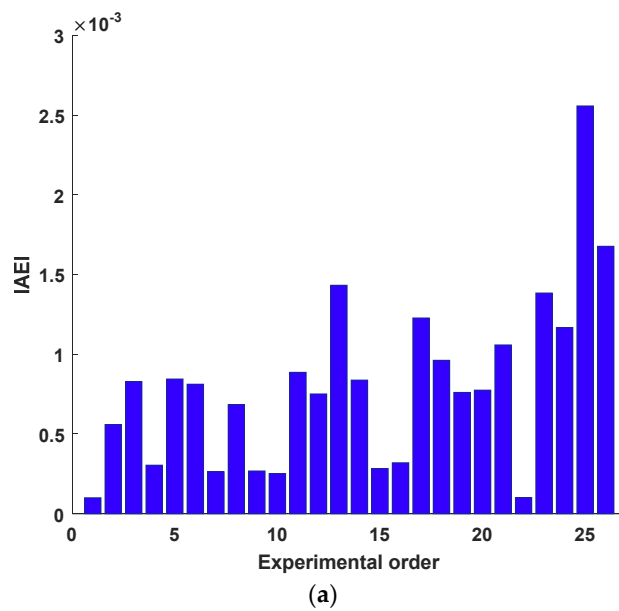
Figure 17. Best RMSE boxplot in 20 individual runs of the MECPO and other recent algorithms for the TDM.

Table 14. Measured and simulated data of voltages, currents, and power and the absolute errors values using MECPO for TDM.

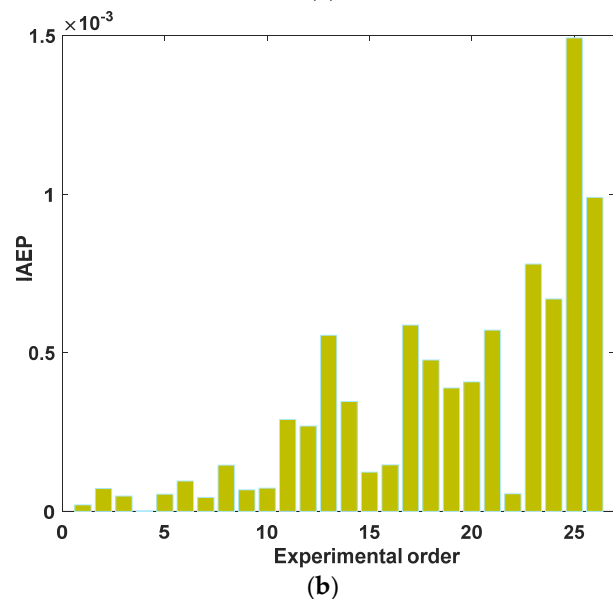
Rank	Experimental Data			Simulated Current Data		Simulated Power Data	
	V (V)	I (A)	P (W)	I_{sim} (A)	IAE_I (A)	P_{sim} (W)	$IAEP$ (W)
1	-0.2057	0.764	-0.157155	0.7639	8.30×10^{-4}	-0.15713	2.00×10^{-5}
2	-0.1291	0.762	-0.098374	0.76256	3.00×10^{-4}	-0.09845	7.00×10^{-5}
3	-0.0588	0.7605	-0.044717	0.76133	8.40×10^{-4}	-0.04477	5.00×10^{-5}
4	0.0057	0.7605	0.004335	0.7602	8.10×10^{-4}	0.00433	$0.00 \times 10^{+00}$
5	0.0646	0.76	0.049096	0.75916	2.60×10^{-4}	0.04904	5.00×10^{-5}
6	0.1185	0.759	0.089942	0.75819	6.80×10^{-4}	0.08985	1.00×10^{-4}
7	0.1678	0.757	0.127025	0.75726	2.70×10^{-4}	0.12707	4.00×10^{-5}
8	0.2132	0.757	0.161392	0.75632	2.50×10^{-4}	0.16125	1.50×10^{-4}
9	0.2545	0.7555	0.192275	0.75523	8.90×10^{-4}	0.19221	7.00×10^{-5}
10	0.2924	0.754	0.22047	0.75375	7.50×10^{-4}	0.2204	7.00×10^{-5}
11	0.3269	0.7505	0.245338	0.75139	1.43×10^{-3}	0.24563	2.90×10^{-4}
12	0.3585	0.7465	0.26762	0.74725	8.40×10^{-4}	0.26789	2.70×10^{-4}
13	0.3873	0.7385	0.286021	0.73993	2.80×10^{-4}	0.28658	5.50×10^{-4}
14	0.4137	0.728	0.301174	0.72716	3.20×10^{-4}	0.30083	3.50×10^{-4}
15	0.4373	0.7065	0.308952	0.70678	1.23×10^{-3}	0.30908	1.20×10^{-4}
16	0.459	0.6755	0.310055	0.67518	9.60×10^{-4}	0.30991	1.50×10^{-4}
17	0.4784	0.632	0.302349	0.63077	7.60×10^{-4}	0.30176	5.90×10^{-4}
18	0.496	0.573	0.284208	0.57204	7.80×10^{-4}	0.28373	4.80×10^{-4}

Table 14. Cont.

Rank	Experimental Data			Simulated Current Data		Simulated Power Data	
	V (V)	I (A)	P (W)	I_{sim} (A)	IAE_I (A)	P_{sim} (W)	IAE_P (W)
19	0.5119	0.499	0.255438	0.49976	1.06×10^{-4}	0.25583	3.90×10^{-4}
20	0.5265	0.413	0.217445	0.41378	1.00×10^{-4}	0.21785	4.10×10^{-4}
21	0.5398	0.3165	0.170847	0.31756	1.38×10^{-4}	0.17142	5.70×10^{-4}
22	0.5521	0.212	0.117045	0.2121	1.17×10^{-4}	0.1171	6.00×10^{-5}
23	0.5633	0.1035	0.058302	0.10212	2.56×10^{-4}	0.05752	7.80×10^{-4}
24	0.5736	-0.0100	-0.005736	-0.00883	1.68×10^{-3}	-0.00507	6.70×10^{-4}
25	0.5833	-0.1230	-0.071746	-0.12556	8.30×10^{-4}	-0.07324	1.49×10^{-3}
26	0.59	-0.2100	-0.1239	-0.20832	3.00×10^{-4}	-0.12291	9.90×10^{-4}



(a)



(b)

Figure 18. Individual absolute errors for current and power by the MECPO for TDM. (a) Individual absolute errors for current. (b) Individual absolute errors for power.

The I-V and P-V characteristics achieved by the proposed technique between the measured data and simulated data are shown in Figure 19. The results obviously show that the simulated data achieved by the MECPO algorithm extremely coincide with the measured data in the different PV models, which means that the identified parameters of the proposed MECPO are highly precise. The above-mentioned comparisons illustrate that the MECPO algorithm has better searching precision, reliability, and more speed convergence rate for determining the parameters extraction problems of various PV models (SDM, DDM, TDM), and its performance is outstanding or competitive in contrast with all other recent techniques.

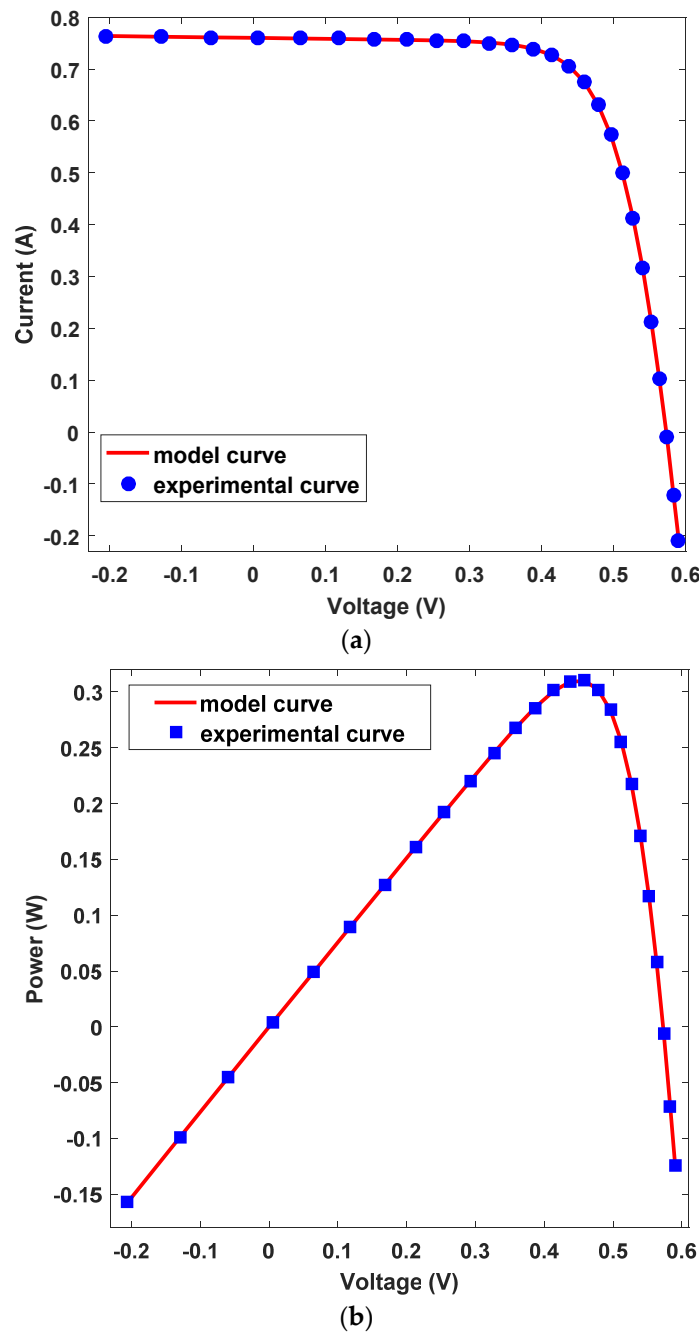


Figure 19. Comparisons between measured data and data achieved using the MECPO method for TDM (a) I-V characteristics and (b) P-V characteristics.

6. Conclusions

This paper has proposed an improved version of the ECPO called MECPO to solve global optimization problems well. This modification has been implemented to escape dropping on the local minima in the conventional ECPO. Therefore, the convergence speed is improved. First, the proposed MECPO's effectiveness has been tested on the different functions of the CEC'17 test suite. The MECPO achieved better performance compared with seven recent optimization algorithms, including GSA, GWO, WOA, SCA, EO, HHO, and the original ECPO. Following that, the suggested strategy based on MECPO has been employed to extract the many parameters of three models of PV cells. An evaluation study is used to test the ability of the MECPO compared with the other optimizers. The comparative study was carried out for the same data set. The statistical results were employed to analyze the efficacy of the MECPO technique. The greatest proximity between the simulated P-V and I-V curves was obtained by the MECPO algorithm in comparison with the measured data. Furthermore, the proposed technique has strong performance and better convergence rates for all tested cases. In future work, the uncertainty of the climate condition as well as the shading effect will be incorporated in the PV models. Additionally, the proposed algorithm is planned to be applied to other fields of energy such as maximum power point tracking (MPPT) and the energy scheduling problem of PV systems.

Author Contributions: Conceptualization, S.K., E.H.H. and M.H.H.; Data curation, M.S. and F.A.H.; Formal analysis, S.K., E.H.H. and M.H.H.; Software, M.S. and F.A.H.; Investigation, S.K., E.H.H. and M.H.H.; Methodology, S.K., E.H.H. and M.H.H.; Project administration, M.S. and F.A.H.; Resources, M.S. and F.A.H.; Software S.K., E.H.H. and M.H.H.; Supervision, E.H.H., M.S. and F.A.H.; Validation, E.H.H. and S.K.; Visualization, M.S. and F.A.H.; Writing original draft, S.K., E.H.H. and M.H.H.; Writing—review & editing, M.S. and F.A.H. All authors have read and agreed to the published version of the manuscript.

Funding: The research received no external funding.

Institutional Review Board Statement: Not applicable.

Informed Consent Statement: Not applicable.

Data Availability Statement: Not applicable.

Acknowledgments: The authors would like to thank Cardiff University/School of Engineering for accepting to pay the APC towards publishing this paper.

Conflicts of Interest: The authors declare no conflict of interest.

References

1. Long, W.; Cai, S.; Jiao, J.; Xu, M.; Wu, T. A new hybrid algorithm based on grey wolf optimizer and cuckoo search for parameter extraction of solar photovoltaic models. *Energy Convers. Manag.* **2020**, *203*, 112243. [[CrossRef](#)]
2. Gnetchejo, P.J.; Essiane, S.N.; Ele, P.; Wamkeue, R.; Wapet, D.M.; Ngoffe, S.P. Enhanced Vibrating Particles System Algorithm for Parameters Estimation of Photovoltaic System. *J. Power Energy Eng.* **2019**, *7*, 94446. [[CrossRef](#)]
3. Deaconu, A.M.; Cotfas, D.T.; Cotfas, P.A. Calculation of Seven Photovoltaic Cells Parameters Using Parallelized Successive Discretization Algorithm. *Int. J. Photoenergy* **2020**, *2020*, 6669579. [[CrossRef](#)]
4. Yeh, W.; Huang, C.; Lin, P.; Chen, Z.; Jiang, Y.; Sun, B. Simplex simplified swarm optimisation for the efficient optimisation of parameter identification for solar cell models. *IET Renew. Power Gener.* **2018**, *12*, 45–51. [[CrossRef](#)]
5. Renewable-Capacity-Statistics. 2021. Available online: <https://www.irena.org/publications/2021/March/Renewable-Capacity-Statistics-2021> (accessed on 9 February 2022).
6. Batzelis, E.I.; Kampitsis, G.E.; Papathanassiou, S.A.; Manias, S.N. Direct MPP Calculation in Terms of the Single-Diode PV Model Parameters. *IEEE Trans. Energy Convers.* **2015**, *30*, 226–236. [[CrossRef](#)]
7. Sharma, A.; Sharma, A.; Averbukh, M.; Jately, V.; Azzopardi, B. An Effective Method for Parameter Estimation of a Solar Cell. *Electronics* **2021**, *10*, 312. [[CrossRef](#)]
8. AlHajri, M.F.; El-Naggar, K.M.; AlRashidi, M.R.; Al-Othman, A.K. Optimal extraction of solar cell parameters using pattern search. *Renew. Energy* **2012**, *44*, 238–245. [[CrossRef](#)]
9. Chellaswamy, C.; Ramesh, R. Parameter extraction of solar cell models based on adaptive differential evolution algorithm. *Renew. Energy* **2016**, *97*, 823–837. [[CrossRef](#)]

10. Louazni, M.; Aroudam, E.H. An analytical mathematical modeling to extract the parameters of solar cell from implicit equation to explicit form. *Appl. Sol. Energy* **2015**, *51*, 165–171. [[CrossRef](#)]
11. Tao, Y.; Bai, J.; Pachauri, R.K.; Sharma, A. Parameter extraction of photovoltaic modules using a heuristic iterative algorithm. *Energy Convers. Manag.* **2020**, *224*, 113386. [[CrossRef](#)]
12. Selem, S.I.; El-Fergany, A.A.; Hasani, H.M. Artificial electric field algorithm to extract nine parameters of triple-diode photovoltaic model. *Int. J. Energy Res.* **2021**, *45*, 590–604. [[CrossRef](#)]
13. Ye, M.; Wang, X.; Xu, Y. Parameter extraction of solar cells using particle swarm optimization. *J. Appl. Phys.* **2009**, *105*, 094502. [[CrossRef](#)]
14. Hassan, M.H.; Kamel, S.; El-Dabah, M.A.; Rezk, H. A Novel Solution Methodology Based on a Modified Gradient-Based Optimizer for Parameter Estimation of Photovoltaic Models. *Electronics* **2021**, *10*, 472. [[CrossRef](#)]
15. Alam, D.F.; Yousri, D.A.; Eteiba, M.B. Flower Pollination Algorithm based solar PV parameter estimation. *Energy Convers. Manag.* **2015**, *101*, 410–422. [[CrossRef](#)]
16. Qais, M.H.; Hasani, H.M.; Alghuwainem, S. Transient search optimization for electrical parameters estimation of photovoltaic module based on datasheet values. *Energy Convers. Manag.* **2020**, *214*, 112904. [[CrossRef](#)]
17. Ma, J.; Ting, T.O.; Man, K.L.; Zhang, N.; Guan, S.-U.; Wong, P.W.H. Parameter Estimation of Photovoltaic Models via Cuckoo Search. *J. Appl. Math.* **2013**, *2013*, 362619. [[CrossRef](#)]
18. Oliva, D.; Abd El Aziz, M.; Ella Hassani, A. Parameter estimation of photovoltaic cells using an improved chaotic whale optimization algorithm. *Appl. Energy* **2017**, *200*, 141–154. [[CrossRef](#)]
19. Xiong, G.; Zhang, J.; Shi, D.; Yuan, X. Application of Supply-Demand-Based Optimization for Parameter Extraction of Solar Photovoltaic Models. *Complexity* **2019**, *2019*, 3923691. [[CrossRef](#)]
20. Messaoud, R. Ben Extraction of uncertain parameters of single and double diode model of a photovoltaic panel using Salp Swarm algorithm. *Measurement* **2020**, *154*, 107446. [[CrossRef](#)]
21. Abdelghany, R.Y.; Kamel, S.; Sultan, H.M.; Khorasy, A.; Elsayed, S.K.; Ahmed, M. Development of an Improved Bonobo Optimizer and Its Application for Solar Cell Parameter Estimation. *Sustainability* **2021**, *13*, 3863. [[CrossRef](#)]
22. Ali, E.E.; El-Hameed, M.A.; El-Fergany, A.A.; El-Arini, M.M. Parameter extraction of photovoltaic generating units using multi-versatile optimizer. *Sustain. Energy Technol. Assess.* **2016**, *17*, 68–76. [[CrossRef](#)]
23. Diab, A.A.Z.; Sultan, H.M.; Aljendy, R.; Al-Sumaiti, A.S.; Shoyama, M.; Ali, Z.M. Tree Growth Based Optimization Algorithm for Parameter Extraction of Different Models of Photovoltaic Cells and Modules. *IEEE Access* **2020**, *8*, 119668–119687. [[CrossRef](#)]
24. Darmansyah; Robandi, I. Photovoltaic parameter estimation using Grey Wolf Optimization. In Proceedings of the 2017 3rd International Conference on Control, Automation and Robotics (ICCAR), Nagoya, Japan, 24–26 April 2017; IEEE: New York, NY, USA, 2017; pp. 593–597.
25. Liao, Z.; Chen, Z.; Li, S. Parameters Extraction of Photovoltaic Models Using Triple-Phase Teaching-Learning-Based Optimization. *IEEE Access* **2020**, *8*, 69937–69952. [[CrossRef](#)]
26. Kanimozhi, G.; Kumar, H. Modeling of solar cell under different conditions by Ant Lion Optimizer with LambertW function. *Appl. Soft Comput.* **2018**, *71*, 141–151. [[CrossRef](#)]
27. Ramadan, A.; Kamel, S.; Hussein, M.M.; Hassan, M.H. A New Application of Chaos Game Optimization Algorithm for Parameters Extraction of Three Diode Photovoltaic Model. *IEEE Access* **2021**, *9*, 51582–51594. [[CrossRef](#)]
28. Jiao, S.; Chong, G.; Huang, C.; Hu, H.; Wang, M.; Heidari, A.A.; Chen, H.; Zhao, X. Orthogonally adapted Harris hawks optimization for parameter estimation of photovoltaic models. *Energy* **2020**, *203*, 117804. [[CrossRef](#)]
29. Premkumar, M.; Babu, T.S.; Umashankar, S.; Sowmya, R. A new metaphor-less algorithms for the photovoltaic cell parameter estimation. *Optik* **2020**, *208*, 164559. [[CrossRef](#)]
30. Kumar, C.; Raj, T.D.; Premkumar, M.; Raj, T.D. A new stochastic slime mould optimization algorithm for the estimation of solar photovoltaic cell parameters. *Optik* **2020**, *223*, 165277. [[CrossRef](#)]
31. Li, S.; Gong, W.; Wang, L.; Yan, X.; Hu, C. A hybrid adaptive teaching–learning-based optimization and differential evolution for parameter identification of photovoltaic models. *Energy Convers. Manag.* **2020**, *225*, 113474. [[CrossRef](#)]
32. Şenel, F.A.; Gökçe, F.; Yüksel, A.S.; Yiğit, T. A novel hybrid PSO–GWO algorithm for optimization problems. *Eng. Comput.* **2019**, *35*, 1359–1373. [[CrossRef](#)]
33. El Sattar, M.A.; Al Sumaiti, A.; Ali, H.; Diab, A.A.Z. Marine predators algorithm for parameters estimation of photovoltaic modules considering various weather conditions. *Neural Comput. Appl.* **2021**, *33*, 11799–11819. [[CrossRef](#)]
34. Diab, A.A.Z.; Sultan, H.M.; Do, T.D.; Kamel, O.M.; Mossa, M.A. Coyote Optimization Algorithm for Parameters Estimation of Various Models of Solar Cells and PV Modules. *IEEE Access* **2020**, *8*, 111102–111140. [[CrossRef](#)]
35. Premkumar, M.; Jangir, P.; Sowmya, R.; Elavarasan, R.M.; Kumar, B.S. Enhanced chaotic JAYA algorithm for parameter estimation of photovoltaic cell/modules. *ISA Trans.* **2021**, *116*, 139–166. [[CrossRef](#)]
36. Naruei, I.; Keynia, F. A New Optimization Method Based on Coot Bird Natural Life Model. *Expert Syst. Appl.* **2021**, *183*, 115352. [[CrossRef](#)]
37. Faramarzi, A.; Heidarinejad, M.; Stephens, B.; Mirjalili, S. Equilibrium optimizer: A novel optimization algorithm. *Knowl. Based Syst.* **2020**, *191*, 105190. [[CrossRef](#)]
38. Harifi, S.; Mohammadzadeh, J.; Khalilian, M.; Ebrahimnejad, S. Giza Pyramids Construction: An ancient-inspired metaheuristic algorithm for optimization. *Evol. Intell.* **2020**, *14*, 1743–1761. [[CrossRef](#)]

39. Faramarzi, A.; Heidarinejad, M.; Mirjalili, S.; Gandomi, A.H. Marine Predators Algorithm: A nature-inspired metaheuristic. *Expert Syst. Appl.* **2020**, *152*, 113377. [[CrossRef](#)]
40. Bouchekara, H.R.E.H. Electric Charged Particles Optimization and its application to the optimal design of a circular antenna array. *Artif. Intell. Rev.* **2021**, *54*, 1767–1802. [[CrossRef](#)]
41. Ismaeel, A.A.K.; Houssein, E.H.; Oliva, D.; Said, M. Gradient-Based Optimizer for Parameter Extraction in Photovoltaic Models. *IEEE Access* **2021**, *9*, 13403–13416. [[CrossRef](#)]
42. Awad, N.H.; Ali, M.Z.; Liang, J.J.; Qu, B.Y.; Suganthan, P.N. *Problem Definitions and Evaluation Criteria for the CEC 2017 Special Session and Competition on Single Objective Bound Constrained Real-Parameter Numerical Optimization: Technical Report*; Nanyang Technological University: Singapore, 2016.
43. Rashedi, E.; Nezamabadi-Pour, H.; Saryazdi, S. GSA: A Gravitational Search Algorithm. *Inf. Sci.* **2009**, *179*, 2232–2248. [[CrossRef](#)]
44. Mirjalili, S.; Mirjalili, S.M.; Lewis, A. Grey Wolf Optimizer. *Adv. Eng. Softw.* **2014**, *69*, 46–61. [[CrossRef](#)]
45. Mirjalili, S.; Lewis, A. The Whale Optimization Algorithm. *Adv. Eng. Softw.* **2016**, *95*, 51–67. [[CrossRef](#)]
46. Mirjalili, S. SCA: A Sine Cosine Algorithm for solving optimization problems. *Knowl. Based Syst.* **2016**, *96*, 120–133. [[CrossRef](#)]
47. Heidari, A.A.; Mirjalili, S.; Faris, H.; Aljarah, I.; Mafarja, M.; Chen, H. Harris hawks optimization: Algorithm and applications. *Futur. Gener. Comput. Syst.* **2019**, *97*, 849–872. [[CrossRef](#)]
48. Arcuri, A.; Fraser, G. Parameter tuning or default values? An empirical investigation in search-based software engineering. *Empir. Softw. Eng.* **2013**, *18*, 594–623. [[CrossRef](#)]
49. Wilcoxon, F. Individual Comparisons by Ranking Methods. In *Breakthroughs in Statistics*; Springer: New York, NY, USA, 1992; pp. 196–202.